Impact of the porosity and moisture state of coarse aggregates, and binder nature on the structure of the paste-aggregate interface: Elementary model study

Duc-Long Tran, Michel Mouret, Franck Cassagnabère

Impact of the porosity and moisture state of coarse aggregates, and binder nature on the structure of the paste-aggregate interface: Elementary model study

Duc Long Tran [a, b, 1], Michel Mouret [a], Franck Cassagnabère [a]

[a] University of Toulouse, UPS, INSA; LMDC, 135 Avenue de Rangueil, Toulouse Cedex 04, France

[b] University of Technology and Education, the University of Danang, 48 Caothang, Danang, Vietnam

Abstract.

The preservation of natural resources and the limitation of CO_2 emissions contribute to sustainable development. In the context of concrete design, this contribution is achieved by using local or recycled aggregates. However, such aggregates can be porous and of low quality, adversely affecting the compressive strength and the durability of concrete. To gain a preliminary understanding, an experimental programme was designed for an elementary model (EM) composed of paste and gravel. This paper analyses the impact of the nature (highly or only slightly porous), the moisture state (saturated surface dry (SSD) or oven dry (OD)) and the volume content of aggregates, together with the binder nature, on i) the water porosity of the EM (WP ^{EM}), and ii) the structure of the paste-aggregate interface. The results indicate that volume and water porosity of the aggregate are the two most important factors affecting WP EM. In order to better highlight the coupling between the nature of the aggregate and the nature of the binder, the porosity of the paste in the EM (WP ^{PEM}) is calculated. This calculation shows that it is the nature of the binder (water retention capacity and reactivity) rather than the aggregate porosity that mainly controls the variations of WP ^{PEM}, in comparison with the porosity of the paste hydrated (WP ^{BP}) without any aggregates. The representation of the difference between WP ^{PEM} and WP ^{BP} by a three-phase model makes it possible to assess the extent of the aggregate disturbance in the arrangement of hydration products (physical thickness of the interfacial transition zone (ITZ)). In most cases this is greater than the chemical disturbance measured with a scanning electron microscope (SEM) in combination with energy-dispersive spectroscopy (EDS). The increase in the aggregate volume content accentuates WP ^{PEM} and the ITZ physical thickness when porous aggregates (natural or recycled) in the SSD moisture state are inserted.

Keywords: Paste-aggregate interface, Metakaolin, Limestone filler, Ground granulated blast furnace slag, Low-calcium fly ash, Water porosity, Moisture state, Interfacial transition zone.

1 Introduction

The design and the production of concrete in the context of sustainable development is now recognized to be a major concern and is increasingly being integrated in construction projects by

[1] Corresponding author

concrete manufacturers, contractors and R&D laboratories. Among the possibilities for reducing the carbon footprint of a concrete design, the replacement of cement with mineral admixture has been under consideration for several years. Not only is the cement content reduced for environmental and economic benefits [1] but the properties of concrete are also most often improved [2]. Another possibility is to use recycled concrete aggregates to preserve natural resources. Over the past ten years, several studies have shown that, provided precautions are taken during the preparation of aggregates (pre-wetting) and during mixing, it is possible to replace part of the natural aggregates in building concrete formulations by recycled aggregates coming from the demolition of concrete structures, without significantly altering the properties of the concrete in the fresh and hardened states [3,4]. In the case of large construction sites that do not have a recycled aggregate production platform nearby, the reduction of transport costs by using local natural aggregates of low quality is also a possibility in the short/medium term.

However, the quality of a concrete depends not only upon the quality of the cement paste and the aggregates, but also on the bond between paste and aggregates. This bond is related to the characteristics of the paste-aggregate interface, named the interfacial transition zone (ITZ), which is, itself, considered as a third phase in mortars and concretes to describe their elastic behaviour [5]. In fact, studies on the ITZ in plain cement-based systems are not recent and the first significant ones date from the 1950s. They have shown that the geometric intimacy of the collage depends on the mineralogical nature of the aggregates [6,7]. In particular, a very close epitaxial contact was observed between dolomitic limestone aggregates and the cement paste. The particular structuring of the ITZ has been progressively highlighted all over the world [8-11]. The ITZ was i) observed as an anisotropic, high porosity area with a thickness of 50-µm on average, in which hydration products of large dimensions are formed, sometimes having a preferential orientation with respect to the aggregate surface, and ii) then considered as the weakest part, controlling the strength and the durability of concrete. Thus, two complementary lines of research have been identified to improve the characteristics of the ITZ. They consist of i) increasing the binding forces between aggregates and hydrates, ii) acting on the crystal growth of hydrates so as to prevent the propagation of cracks through the hydrates and to increase the cohesion of the paste in the vicinity of the aggregates [12]. Over the years, many studies have identified several concrete design factors on which to act to improve the structure of the ITZ. A decrease in the ITZ porosity can be achieved by i) decreasing the water/binder ratio [13-15], ii) using the saturated surface dry (SSD) moisture state of aggregates [16] with smooth rather than rough surface texture [17], and iii) decreasing the aggregate size [18]. The increase in the volume of aggregates at a constant specific area increases

the ITZ volume which, in turn, can have a negative effect on the Young's modulus of the mortar and concrete [19]. The incorporation of mineral admixtures is another factor that noticeably influences the structure of the ITZ. Fly ash [20-21], silica fume [14,22-24], and metakaolin [2,25] have a positive densifying effect on the ITZ and, as pozzolans, reduce the amount and decrease the orientation of calcium hydroxide. The difference between the ITZ and the bulk paste properties is then reduced and the quality of the ITZ can even be enhanced with the decrease in the particle size of the mineral admixture [14]. As a latent hydraulic mineral admixture, blast furnace slag also has some positive effects on the ITZ characteristics by decreasing the amount of crystals at the paste-aggregate interface [26] and, particularly, the build-up of calcium hydroxide [27]. Limestone filler is reported to have a densifying effect on the ITZ, by its physical filling ability [28] and its chemical reactivity [29].

It is important to note that all the above results were obtained with slightly porous or non-porous aggregates, whether the related studies were based on composite specimens (paste cast against a plane rock surface) or real cement-based materials (mortars, concretes). In fact, very limited information is available with respect to the interface between cement-based matrixes and aggregates with significant open porosity. When pre-wetted lightweight aggregates (LWA) with a porous outer layer are used, the ITZ is more dense and homogeneous than that observed in normal weight, aggregate-based material [30]. It even seems that the moisture state of the LWA (dried or pre-wetted) has little influence on the microstructure of the ITZ [31], which is observed to be denser and thinner than that developed on normal aggregate. In the case of recycled concrete aggregates (RCA), for which the high open porosity is due to the remaining cement paste that partially covers them, the results depend on the moisture state. No difference is noticed between the paste close to or far from the RCA when it is incorporated in a dry state [32]. In oversaturated conditions and in the case of 1-year-old concretes with moderate water/cement ratio (> 0.4), the water release from the RCA implies a higher porosity and less anhydrous phase over a distance of 100 µm from the aggregate in comparison with natural aggregates [33]. Hence, the efficiency of the water release from porous aggregate to the cement-based matrix, namely the internal curing, defined as having a positive effect on concrete properties when LWA is incorporated [34] is dependent on the content and the nature of the porous aggregate, particularly on its surface texture related to the size of the open pores.

This paper is the first part of a large study dealing with the influence of the intrinsic porosity of coarse aggregates on the properties of normal-strength concrete. Here, the objective is to characterize the paste-aggregate interface in a composite specimen, named the elementary model

(EM), according to the nature, properties and moisture state of aggregates, the volume content of aggregates, and the nature of the binder in contact with the aggregates. Even though the interfaces in composite specimens may not be representative of the paste-aggregate interfaces in real concrete [35,36], they can be considered as giving a preliminary view towards understanding the phenomena occurring in concrete. Hence, by considering some factors identified in the literature mentioned above and recognized as affecting the ITZ, some comparative data between porous and non-porous aggregates are provided by investigating the paste-aggregate interface from the physical and chemical points of view.

2 Experimental procedure

The study was conducted on an elementary model (EM) consisting of the association between cementitious paste and gravel. The parameters investigated were the water porosity (WP), the moisture state and the volume of coarse aggregates, and the nature of the binder. Five kinds of aggregates (more and less porous), two moisture states (oven-dry (OD) and saturated surface dry (SSD)) and four kinds of mineral admixtures (metakaolin, limestone filler, slag and fly ash) were studied. The properties measured on the hardened EM samples were the water porosity (WP^{EM}) and the elemental chemical analysis at the paste-aggregate interface for the evaluation of the chemical width of the interfacial transition zone (e^{M}_{ITZ}).

2.1 Materials

2.1.1 Raw materials

The cement used was an Ordinary Portland Cement, CEM I 52.5N according to European standard NF EN 197-1 [37]. The metakaolin (MK), complying with the French standard NF P18-513 [38] for pozzolanic mineral admixtures for mortar and concrete, was produced by flash calcination of kaolinite clays. The limestone filler (LF) came from the mechanical grinding of pieces of rock extracted from a quarry and usable for concrete applications according to the French standard NF P18-508 [39]. The slag (GGBS) was produced by drying and grinding the granulated blast furnace slag and met the specifications of European standard NF EN 15167-1 [40]. The low-calcium fly ash (FA), compliant with European standard NF EN 450-1 [41], came from a thermal power plant. Table 1 shows the main chemical and physical properties of the cement and the four mineral admixtures used. The size distributions of the powders (laser diffraction, wet dispersion) are presented in Fig. 1.

Table 1. Main characteristics of cement and mineral admixtures

	Cement I 52.5 N	Metakaolin (MK)	Limestone filler (LF)	Slag (GGBS)	Fly ash (FA)
Physical characteristics					
Density (g/cm^3)	3.09	2.50	2.70	2.90	2.00
Specific surface area (cm^2/g)	4600 (Blaine)	160000 (BET)	5960 (Blaine)	4450 (Blaine)	2300 (Blaine)
D_{50} (µm)	16.0	30.0	5.5	11.0	30.0
Chemical / Mineralogical composition (wt. %)					
SiO_2	20.1	67.80	/	37.4	52.5
Al_2O_3	5.2	25.36	/	10.8	22.5
Fe_2O_3	3.3	2.30	/	0.5	8.5
CaO	64.1	0.36	/	43.7	3.5
$CaCO_3$	/	/	95	/	/
Na_2Oeq	0.78	/	/	/	/

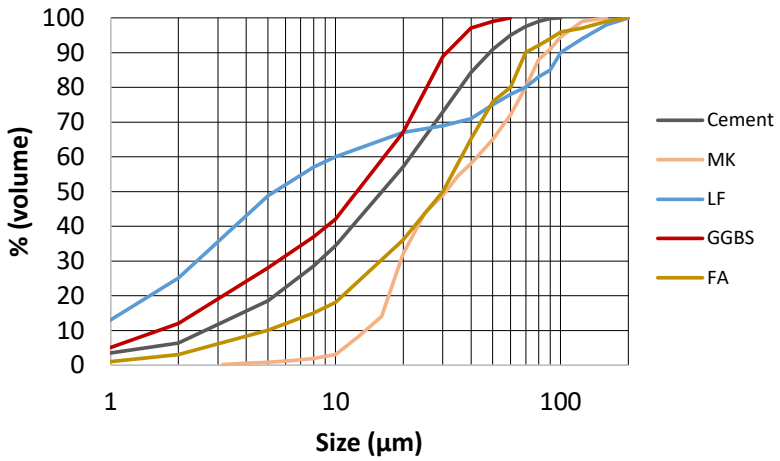

Fig. 1. Volume distribution of particle size of the powders (laser diffraction, wet dispersion)

It is important to notice that metakaolin presents a coarse particle size distribution (Fig. 1). This observation is due to the flash calcination process and a high impurity rate, particularly pertaining to quartz particles.

Five types of coarse aggregate were used. They were classified in two groups:

- Low porosity aggregates G1, G2 and G3, differing mainly by their mineralogical nature: totally siliceous (G1), or totally calcareous (G2) or siliceous-calcareous (G3);
- Porous aggregates G4 and RA, differing by their origin, either natural (G4) or recycled from demolished concrete structures (RA).

The main properties of the aggregates are presented in Table 2, which shows that the average values of the open porosity are of the same order as the ones related to the 24-h water absorption,

thus validating the two groups defined above. The first one gathers together three slightly to non-porous aggregates (G1, G2 and G3) with 24-h water absorption coefficient less than the most severe specified value of the French standard NF P18-545 [42] for concretes and mortars (2.5%). The second one includes two porous aggregates (G4 and RA) with 24-h water absorption coefficient significantly greater than 2.5%.

Table 2. Characteristics of the aggregates

	Designation	Density * (kg/m^3)	Water porosity ** (vol. %)	24-h water absorption * (wt. %)	Mineralogy (>90% by mass)
G1	Siliceous-quartz	2600	0.7 ± 0.3	0.5	SiO_2 (quartz)
G2	Hardened limestone	2670	0.9 ± 0.4	0.6	$CaCO_3$ (calcite)
G3	Siliceous-calcareous	2590	1.2 ± 0.7	1.0	Quartz, calcite
G4	Soft limestone	2420	12.5 ± 2.1	4.2	Calcite
RA	Recycled	2260	20.0 ± 1.8	5.2	Multi-phases

* *Supplier data in accordance with French Standard NF EN 1097-6* [43].

** *Measurement according to French standard NF P18-459* [44] *(see Section 2.3).*

Average ± standard deviation (ten measurements – for one measurement, ten particles, each belonging to the size class [14-16]mm were tested).

2.1.2 Elementary Model (EM)

Each elementary model (EM) sample was in the form of cylinders (5cm-diameter and 4cm-height, on average) and was made with a fixed volume of cement-based paste and various volumes of coarse aggregates.

a) Apparent volume content of aggregate V^{agg} and moisture states.

The apparent volume of coarse aggregate, V^{agg}, (measurement protocol described in section 2.3.1) was varied by $3.30cm^3 \pm 0.05$, or $7.30cm^3 \pm 0.05$ or $9.80\ cm^3 \pm 0.05$, which corresponded, for the grading distribution of a given aggregate, to two, four or six selected gravels in the size class [14-16] mm being incorporated in the paste. The aggregates were chosen visually in the size class so that their shape was as rounded as possible. In addition, by setting that $V^{agg} = V$ in the case of two aggregate particles in EM, then the notation $V^{agg} = 2V$ or 3V will be used subsequently to denote the apparent aggregate volume content corresponding to 4 or 6 particles in EM, respectively. The Saturated Surface Dry (SSD) moisture state was obtained according to the measurement protocol described in Section 2.3.1. The oven dry (OD) moisture state was achieved

after three days at 105°C for natural aggregates (G1, G2, G3 and G4) and after 7 days at 50°C for recycled aggregates (RA). The pre-conditioning to target RA in the OD moisture state was chosen to avoid destruction and microcracking of the hydrated phase enveloping part of the parent aggregate (from 20% to 30% by volume, measured by successive microwave heating, up to the visual aspect of natural aggregate).

b) Binders and composition of the pastes.

Five compositions of binder (cement + mineral admixture) were considered (Table 3). The reference composition was only cement (B1), while the other four were made by replacing cement with 15% metakaolin (B2), or 25% limestone filler (B3), or 30% slag (B4) or 30% fly ash (B5) by mass according to the maximum replacement rates fixed by the European standard NF EN 206/CN [45]. The water/binder ratio (W/B) was fixed at 0.35, which made it possible to:

- obtain a paste of plastic consistency enabling the immersion of the aggregates without segregation at rest (for all pastes, the static yield stress was measured and was greater than the minimum value corresponding to the balance between the forces acting on an aggregate particle of given size suspended in the paste),
- satisfy the minimum water demand of the binders previously measured at a transitional state from coherent packing (humid soil) to a concentrated suspension (thick paste) [46].

Table 3. Composition of the pastes (reference to a 0.5 litre batch of B1)

Designation	Composition of binder (% mass)	Cement (g)	Mineral admixture (g)	Water (g)
B1	100% cement	750.0	0.0	262.5
B2	85% cement + 15% MK	637.5	112.5	262.5
B3	75% cement +25% LF	562.5	187.5	262.5
B4	70% cement + 30% GGBS	525.0	225.0	262.5
B5	70% cement + 30% FA	525.0	225.0	262.5

Higher (W/B) ratios as those encountered in the current concrete practice ($0.45<W/B<0.65$) have not been investigated. Such values would lead to unstable suspensions at the EM scale and given the number of specimens studied (Section 2.2), they would require too heavy experimental adaptations such as continuous stirring until the cement sets.

2.2 Casting, moulding and curing of EM samples

For a given binder, a one-litre batch was prepared by means of a standard mixer complying with European standard NF EN 196-1 [47]. The mixing sequence was always as follows:

- Dry-mixing of cement and mineral admixture for 1 minute at low speed.
- Addition of water during mixing for 0.5 minute.
- Mixing continued for 1 minute at high speed and 1 minute at low speed.

The total mixing duration was 3.5 minutes.

Immediately after mixing, a given volume of aggregate (1V or 2V or 3V) in the SSD or OD moisture state was added into a fixed volume of fresh paste (42.40 $cm^3 \pm 0.90\ cm^3$) in a cylindrical mould (5 cm in diameter and 4 cm in height) (Fig. 2). Then, each EM was homogenized by 5s vibration by means of a vibrating table (50 Hz, 1g). Finally, EMs were sealed for the first 24 hours and stored at 20°C ± 2°C, then demoulded and cured by immersion in water at 20°C ± 1°C for 90 days. Various saw cuts of the EM samples in the hardened state made it possible to verify that the aggregates were separated by at least 1 mm from each other and were also located more than 1mm from the edges of the sample. Four hundred and fifty EMs were composed in total, from five kinds of binder, five kinds of aggregates, two moisture states and three volumes of aggregates, in addition to a 3-times repeatability.

Simultaneously with EMs, other samples were made and cured using the same protocol as that applied above:

- Paste samples with binder only (three samples/binder) in order to measure the water porosity, WP^{BP}, and the volume of the bulk paste in the hardened state. It is important to note that the volume of the fresh paste used to measure WP^{BP} was the same as the one used to make the EM samples.
- EM samples with one volume of aggregates (one sample/(SSD or OD aggregate-binder) combination) in order to characterize the chemical width of the aggregate-paste interface (Section 2.3.2).

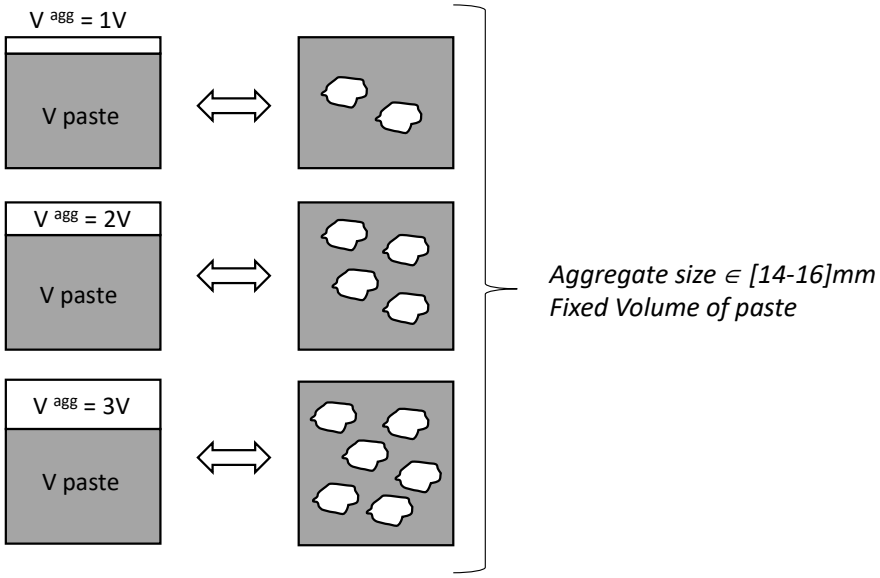

Fig. 2. Schematic representation of the elementary model EM in the fresh state – volume scheme (left), number scheme (right)

2.3 Tests

2.3.1 Water porosity (WP)

There are several methods available to measure the connected or open porosity of materials among which figures the gravimetric method by liquid impregnation, where, for a given solid nature, the results depend on the choice of the liquid. If the liquid wets the solid poorly, it will not be able to penetrate into the pores completely and, if it wets the solid very well, it will tend to penetrate into all the pores accessible to its molecules. In this case, an increase in open porosity is expected as the size of the probe molecule decreases. In France as elsewhere around the world, there are two separate standards, dedicated to the measurement of the open porosity of rocks and hardened cement-based materials, respectively. Since such materials are hydrophilic, both methods are based on water impregnation and are not very different from each other regarding the operating procedure. The protocol consists of saturating the material with water and then drying it. Hence, the French standard NF P18-459 [44] for the measurement of the open porosity of hardened cementitious materials was applied to both aggregates and hardened EM samples.

1) The samples (aggregates or EM (entire cylinder sample 5 cm in diameter and 4 cm high)) after the curing period, or paste samples after the curing period) were placed in a desiccator under vacuum (24 mbars) for 4 hours and then saturated in water under vacuum for 48 hours (this step also corresponded to the SSD moisture state for aggregates to be incorporated into the paste).

2) Next, the samples were weighed while submerged (hydrostatic weighing, M_{water}), and then weighed in the air (M_{air}) after their surface had been wiped with a damp cloth.
3) Finally, the samples were dried at 105°C ± 5°C in a ventilated oven until a constant mass, M_{dry}, was reached (no more than 0.1% difference between two successive weighings performed 24 hours apart).

During steps 1) and 2), the water temperature was 20°C ± 2°C.

The open porosity WP^{i} (%) was calculated according to Eq. (1):

$$WP^{i} = \frac{M_{air} - M_{dry}}{M_{air} - M_{water}} . 100 = \frac{V_V{}^{i}}{V^{i}} .100 \quad (1)$$

where: $V_V{}^{i}$ and V^{i} are the volume of open pores and the apparent volume, respectively (i = agg for aggregates, i = EM for elementary model, i = BP for bulk paste).

By using Eq. (1), the open porosity of aggregates, WP^{agg}; the elementary model, WP^{EM}; and bulk paste (paste samples with binder only), WP^{BP}, could be calculated.

2.3.2 Chemical width of ITZ (e^{M}_{ITZ})

An investigation was made on the aggregate-paste interface to assess the width of the interfacial transition zone. To that end, after 90 days of water curing, the EM samples were sawn in the direction of the immersion of the aggregates, and gently dried. Next, they were impregnated with an extremely low viscosity resin (in cylindrical plastic moulds 2 cm in diameter and 1.8 cm in height) and the tested surface was polished (Fig. 3) after 24 hours' curing in the atmosphere. After dry polishing, the tested surfaces of the samples were cleaned with ethanol and coated with carbon (30 nm) for observation. The scanning electron microscope (SEM) in backscattered electron mode (BSE imaging) was used in combination with Energy Dispersive Spectroscopy (EDS) in order to carry out an elemental analysis through 100 aligned point scans starting from the aggregate phase and ending with the bulk paste, on the polished sections (Fig. 3). Ten line scans (110 µm in length) were conducted for each sample (Fig. 4).

Several works reported in literature have shown that the nucleation and development of Portlandite crystals on the aggregate surface (often called "duplex film") and in the vicinity of aggregates are more pronounced than in the bulk paste [9,48]. Accordingly, and due to high calcium content of the CSH phase in the aggregate vicinity, the overall Ca/Si molar ratio gradually declines with the increasing distance from the aggregate [49]. In line with these previous results, the chemical width of the interfacial transition zone (e^{M}_{ITZ}) was determined, based on variation of the Ca, Si and Ca/Si atomic ratios, as illustrated in Fig. 5.

Fig. 3. SEM-EDS polished samples of EM

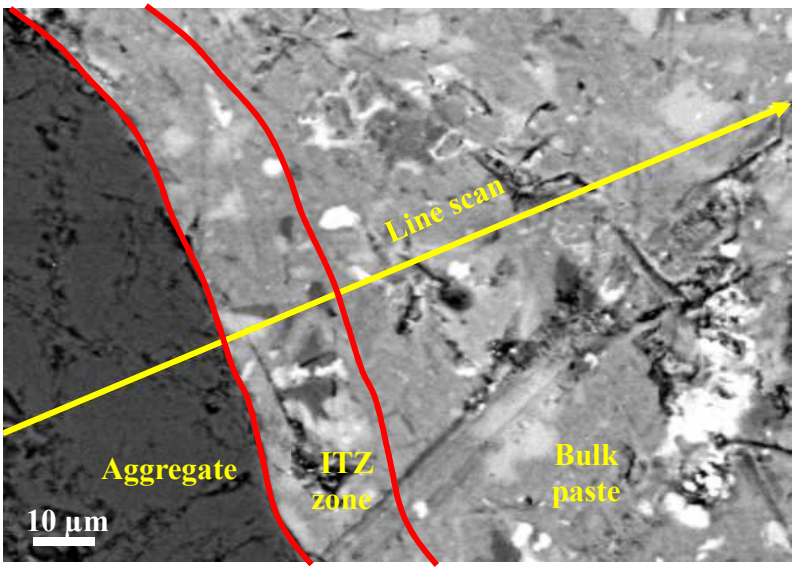

Fig. 4. Illustration of the line scan method (BSE imaging)

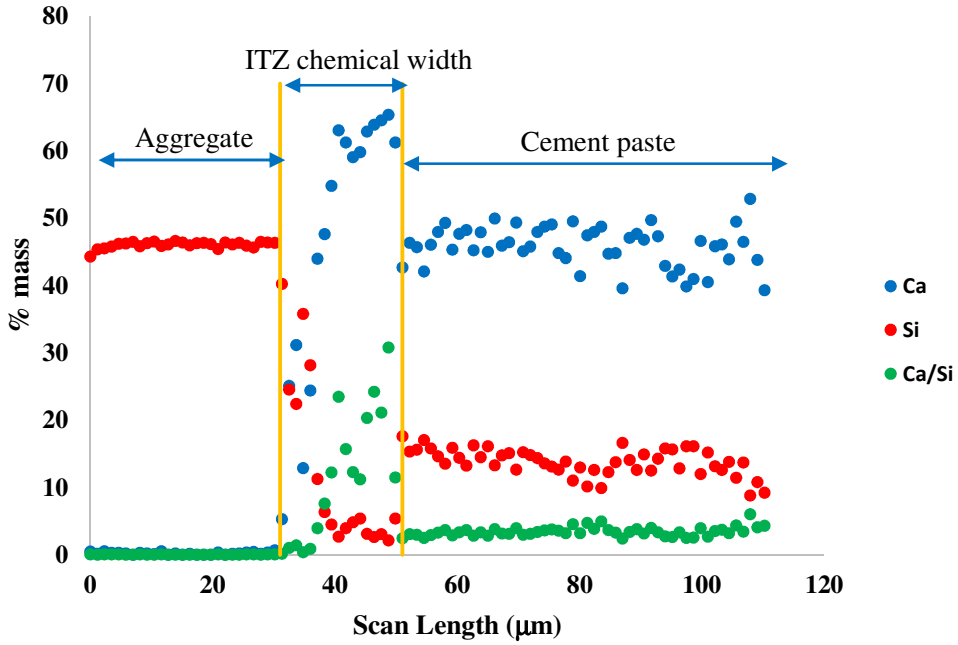

Fig. 5. Typical identification of the ITZ chemical width e^{M}_{ITZ} from the line scan method by SEM/EDS – G1(OD) aggregate combined with B3 binder

3 Raw results

3.1. Water porosity of elementary model: WP ^{EM}

A typical evolution of the open porosity of the elementary model, WP ^{EM}, as a function of the apparent volume content of aggregates (V ^{agg}) is shown in Fig. 6 for porous and non-porous aggregates in SSD and OD moisture states.

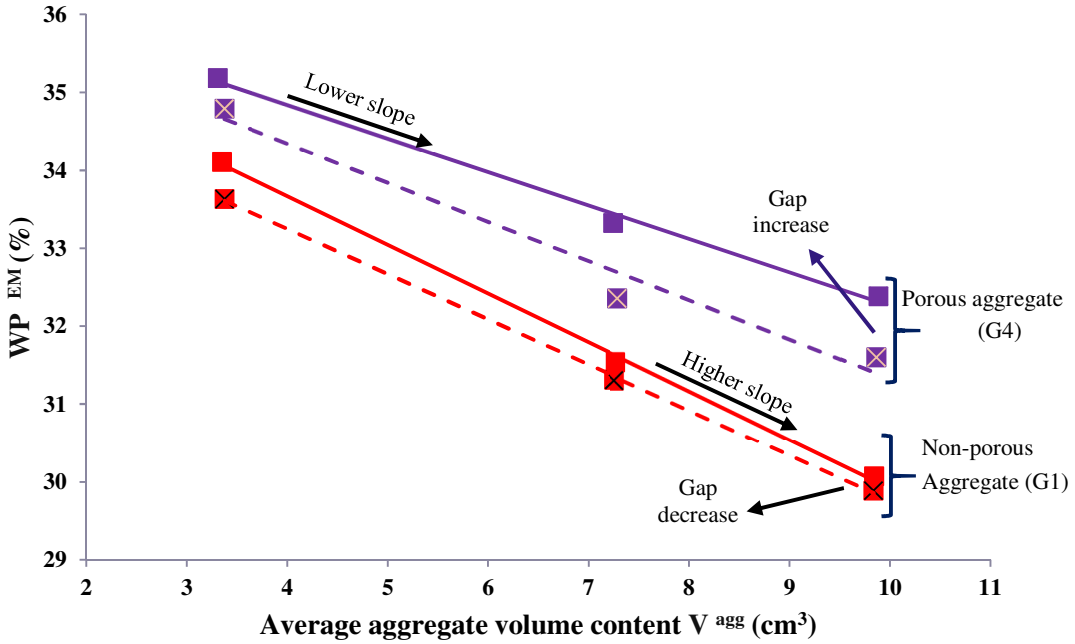

Fig. 6. Typical evolution of WP ^{EM} versus the aggregate volume for porous (G4) and non-porous (G1) aggregates with binder B1 in OD (dotted line) and SSD (full line) moisture states

As expected, WP ^{EM} decreased when V ^{agg} increased: the paste porosity (>30%, see Section 4.1.3, Fig. 10) was significantly higher than the aggregate porosity (≤20%), while the volume proportion of paste and aggregates decreased and increased, respectively. However, the more marked slope decrease in specimens with non-porous aggregates than in those with porous ones expressed a modification of the paste porosity depending on the aggregate porosity, WP ^{agg}. Furthermore, the gap between the linear tendencies in SSD and OD states was greater for porous aggregates than for non-porous ones, which highlights a marked influence of the moisture state and WP ^{agg} on WP ^{EM} when porous aggregates are incorporated. It is also important to note that this gap tended to increase (decrease) when V ^{agg} of porous (non-porous) aggregates increased, which highlights the importance of the effect of volume of the paste-aggregate interface on the results.

Based on the Kendall's coefficient of concordance, W, (Eq. (2)) [50], a ranking analysis of all the results showed WP^{EM} classified in the same order as WP^{agg}, whatever the nature of the binder, the moisture state and the volume of aggregates. As shown in Table 4, in all cases, Kendall's coefficient of concordance (W) was higher than the threshold at the 0.01 significance level.

$$W = \frac{12.S}{k^2.(n^3-n)-k\sum_1^k(\sum_1^s(t^3-t))} \quad (2)$$

with: S : variance of the sums of ranks;

k : number of judges (five binder natures);

n : number of contestants (five aggregate natures);

t : tie corresponding to a set, s, of ranks for a given judge (tie was considered in the case of non-significant differences between WP^{EM} average values, given their respective standard deviation values).

Table 4. Kendall's coefficient of concordance W values

Moisture state of aggregate	Aggregate volume	W	Threshold at 0.01 significance level
SSD	1V	0.808	0.571
	2V	0.956	
	3V	0.961	
OD	1V	0.632	
	2V	0.755	
	3V	0.633	

Thus, the statistical ranking analysis confirmed the overall dependence of WP^{EM} on WP^{agg}. However, this dependence can hide the effect of the coupling, between the nature of the aggregate and the nature of the binder for a given moisture state of the aggregate, on the structuring of the hardened paste around the aggregates.

Analysis of the porosity of the matrix of EM samples will be developed in Section 4.1, according to the nature, volume content and moisture state of the aggregate, and the nature of the binder.

3.2. Chemical width of the paste/aggregate interface: e^{M}_{ITZ}

The e^{M}_{ITZ} was measured according to the procedure detailed in Section 2.3.2. For a given aggregate/binder combination and a given aggregate moisture state, the average and the standard deviation values are gathered together in Table 5, which also shows the median size values of the binders. They were determined from the size distribution of each binder and are known with a 2 µm uncertainty.

Table 5. e^{M}_{ITZ} (mean ± standard deviation) and median size of the binders (µm)

	G1		G2		G3		G4		RA	
	SSD	OD	SSD	OD	SSD	OD	SSD	OD	SSD	OD
B1	21.0	17.5	13.0	12.5	14.0	13.5	9.5	9.0	13.0	10.0
16.0(*)	±4.5	±3.5	±1.5	±1.0	±2.0	±1.5	±1.5	±1.0	±1.5	±1.5
B2	19.0	17.5	18.0	18.5	14.5	12.5	15.0	14.0	14.5	11.0
19.0(*)	±4.0	±2.0	±2.5	±1.5	±1.5	±2.5	±2.0	±2.5	±1.0	±2.5
B3	19.5	17.5	18.5	12.5	14.5	10.0	17.0	17.0	19.5	11.5
14.0(*)	±1.5	±3.0	±1.5	±3.5	±2.0	±1.0	±2.0	±3.5	±2.5	±2.5
B4	15.5	18.0	15.0	16.5	14.5	13.5	15.0	17.5	13.5	20.0
15.0(*)	±2.5	±2.0	±3.0	±2.0	±3.0	±2.0	±1.0	±1.0	±2.0	±3.0
B5	12.0	21.0	12.0	16.5	9.5	17.0	12.5	17.5	13.0	20.0
20.0(*)	±1.5	±3.5	±2.0	±2.0	±2.0	±3.0	±2.0	±1.0	±1.5	±2.0

(*) *Median size of the binder (µm)*

Globally, as shown in Table 5, the mean values range from 9.0 µm to 21.0 µm. Through the wall effect of the aggregate, which is larger than the cement grains, it was shown that the ITZ thickness can be associated with the median size of the cement grains, typically before any hydration, and tends to fall below this median size as hydration proceeds [14]. Hence, if we extend this finding to the median size of binders in the present study, the e^{M}_{ITZ} values are of the same order of magnitude as the median size of the binders or are significantly smaller. The values greater than the median binder size (3/50) are exclusively observed for the binder B3 (cement + limestone) associated with SSD recycled aggregate (RA) and SSD nonporous aggregate (G1, G2). This observation may be due to the presence of a significant amount of limestone filler, which contributes to an increase in the Ca/Si ratio in the EM samples and to confusion with hydration products such as Portlandite.

In addition, by applying the ranking statistical analysis in the same way as in Section 3.1, it can be concluded that i) the e^{M}_{ITZ} values in EM samples are not ranked in the same order as the aggregate porosity (WP^{agg}), ii) the ranking depends on the nature of the binder for a given moisture state of the aggregates. The dependence of the chemical thicknesses on the nature of the binder is particularly marked when the values are compared according to the aggregate moisture state. The binder B5 (cement + fly ash) leads to systematically higher values when associated with OD aggregates than with SSD aggregates, porous or not. This observation is found again when binder B4 (cement + slag) is associated with porous aggregates (G4, RA). Conversely, the binder B3

(cement + limestone filler) combined with nonporous (G2, G3) or porous (RA) aggregates develops higher e^{M}_{ITZ} values in the SSD state than in the OD state.

Based on the variation in the calcium content from the aggregate surface to the bulk paste, the e^{M}_{ITZ} expresses the formation of various calcium-based hydration products close to the aggregate surface, depending on the nature of the binder and the intensity of the movement of water from the paste towards the aggregates at early ages. Even though the thicknesses measured seem to be supported by literature data, they are not directly linked to the water porosity values of EM, WP^{EM} (Fig. 7). Furthermore, the literature reports a variety of ITZ thicknesses that actually depend on the type of aggregate and binder used, the water / binder ratio of the mixture, the age of the material, and the method used to characterize it. Values up to 100 µm were recorded on hardened C_3S-marble systems by Ca / Si ratio measurement using electron probe micro-analysis [49].

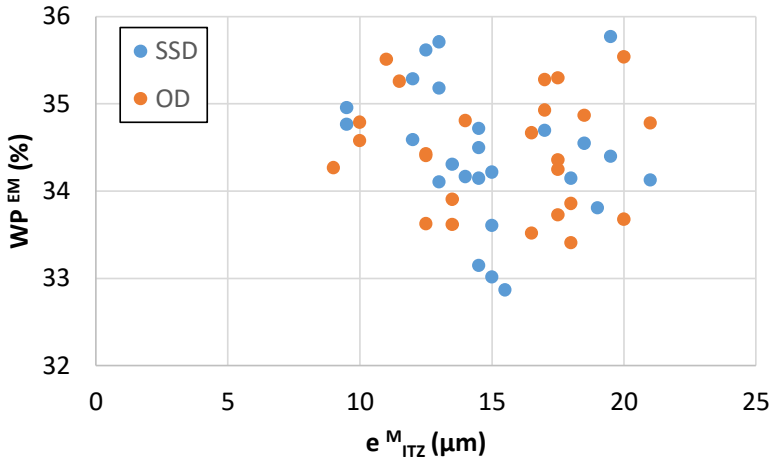

Fig. 7. Water porosity of EM samples versus ITZ chemical width (e^{M}_{ITZ})

It is therefore legitimate to question the physical relevance of the e^{M}_{ITZ} indicator in structuring the paste near the aggregates because the porosity results can reflect the influence of the aggregates on the arrangement of the hydration products in the paste. This point will be discussed in detail in Section 4.2.

4 Analysis and discussion

In this section, the porosity results are transformed by eliminating the presence of aggregates. The porosity of the paste of the samples of EM, WP^{PEM} is thus obtained (Section 4.1). The comparison between WP^{PEM} values and the porosity of the bulk paste measured in samples containing no aggregate, WP^{BP}, will then make it possible to give a physical representation of the extent of the interfacial zone between paste and aggregates in EMs (Section 4.2).

4.1 Water porosity of the paste of EMs: WP^{PEM}

4.1.1. Expression for WP^{PEM}

Let X be the volume fraction of aggregate open pores that are not filled, either with water or with paste. Then, WP^{EM} can be developed (Eq. (3)):

$$WP^{EM} = \frac{V_V^{EM}(X)}{V^{EM}} = \frac{X.V_V^{agg} + V_V^{PEM}(X)}{V^{EM}} \quad (3)$$

where V_V^{EM}, V_V^{agg}, V_V^{PEM} and V^{EM} are the volume of open pores of EM, the volume of open pores of aggregates, the volume of open pores of the paste of EM and the apparent volume of EM, respectively.

Since the volume of aggregates in EM samples, V^{agg}, is known, and since water porosity of aggregates, WP^{agg}, has been measured, it is possible to write Eq. (4):

$$WP^{EM} = \frac{X.V^{agg}.WP^{agg} + V_V^{PEM}(X)}{V^{EM}} \quad (4)$$

In parallel, it is possible to express the water porosity of the paste contained in EM samples, WP^{PEM}, as Eq. (5):

$$WP^{PEM}(X) = \frac{V_V^{PEM}(X)}{V^{PEM}(X)} \quad (5)$$

where V^{PEM} is the apparent volume of the paste of EMs. V^{PEM} can be developed as the difference between the apparent volume of EM and the apparent volume of aggregates comprising only the unfilled open pores (Eq. (6)):

$$V^{PEM}(X) = V^{EM} - V^{agg}.[1 - WP^{agg}.(1 - X)] \quad (6)$$

By expressing V_V^{PEM} by means of Eq. (4) and considering Eq. (6), WP^{PEM} (Eq. (5)) can be written in a more explicit form (Eq. (7)):

$$WP^{PEM}(X) = \frac{WP^{EM} - X\Gamma_{agg}WP^{agg}}{1-\Gamma_{agg}[1-WP^{agg}(1-X)]} \quad (7)$$

where Γ_{agg} is the volume fraction of aggregate in the EM $\left(\text{i.e. } \frac{V^{agg}}{V^{EM}}\right)$.

Finally, the effect that coupling the aggregate nature and binder nature has on the paste of EM (PEM) can be highlighted by comparing WP^{PEM} values (Eq. (7)) with the water porosity values of the bulk paste, WP^{BP}, measured on samples that did not incorporate aggregates (Sections 2.2 and 2.3.1).

In Eq. (7), WP^{EM} and WP^{agg} are obtained from measurements (Eq. (1), see Section 2.3.1). The aggregate volume fraction, Γ_{agg}, is also known since V^{agg} and V^{EM} are measured. Accordingly, WP^{PEM} can be calculated if the volume fraction of aggregate open pores unfilled in the hardened

90-day EM, X, is known. The next section justifies the value chosen for X in order to evaluate WP^{PEM} correctly with Eq. (7).

4.1.2. Is the volume of aggregate open pores fully or partially filled with hydrated paste in the 90-day EM samples?

The following discussion starts from the fresh state of the EM samples and considers a function of the moisture state of the aggregates (OD or SSD).

In the OD condition, the pores of the aggregates immersed in the paste immediately after mixing will fill with water extracted from the paste under the action of capillary forces. According to the laws of absorption by capillarity, the penetration velocity of a liquid in a capillary tube is proportional to the square root of the radius of the tube [51], so the large capillaries will fill up first. Considering the threshold size of 0.1µm that usually distinguishes the capillary porosity (>0.1µm) and the hydration products porosity (<0.1µm) in cement-based paste, the volume of the capillaries in aggregates represents from 80% (limestone porous aggregates with porosity >30% [52] to 95% (low porous quartz aggregates with 24-h water absorption <1.5% [53] of the total accessible pore volume. Hence, it can be considered that the capillary porosity is predominant in the natural aggregates studied. The porosity of recycled aggregates (RA) depends on the porosity of the natural parent aggregates and that of the attached mortar that partially covers them. The porosity of the attached mortar itself depends on the design and properties of the original concrete. Assuming that the capillary porosity of the mortar represents at most 50% of its total porosity for water/cement ratios ranging from 0.45 to 0.60 [54], and considering the volume percentage of the mortar in the RA (Section 2.1.2a), the capillaries in RA can also reach 80% of the total accessible pore volume. Thus, the capillary porosity in RA is predominant.

In parallel, unlike water in the free surface condition prevailing in Jurin's law, the water contained in a fresh cementitious paste is subject to physical and chemical forces and, in particular, to capillary forces. During mixing, the voids existing between the binder grains are filled with water. As the first hydration products precipitate, the size of the paste capillaries decreases. The aggregates immersed in the paste absorb water, which has the effect of tightening the grains together and further reducing the size of the paste capillaries. It follows that water retention in the paste increases as the time elapsed since mixing increases. The suction of the aggregates therefore decreases over time. Accordingly, in the first moments of the immersion of the aggregates in the paste, the large, open pores of aggregates can extract water from the paste by capillary action and, subsequently, when the time after mixing increases, only the small pores become impregnated with water. The impregnation of small aggregate pores is possible provided that they are at least of

smaller size than the pores existing in the paste, as demonstrated by a previous study of the effect of porosity properties (volume and size distribution) in porous substrates (natural minerals, clay ceramics) on cement paste up to 90 minutes after mixing [55]. Moreover, Grandet's study [55] has shown that the binder properties, specifically its specific surface area and its size distribution, also have an influence on the rate of impregnation of porous aggregates. This rate decreases when the specific surface area and the amount of coarse particles increase, i.e. when the size and the number of capillaries decrease, respectively. The increase in the coarse particle content in the binder decreases the number of paths between the paste and the aggregate, thereby enhancing the water retention of the paste. Another important result of the previous study is the influence of the water /binder ratio of the paste on the behaviour of a porous mineral in contact with a cementitious paste. The values investigated were less than 0.3. However, in the present study, this ratio was kept constant at 0.35 (see Section 2) and undoubtedly favoured the suction of large quantities of the interstitial free aqueous phase from the fresh paste towards the aggregates, which helped to saturate them. The saturation could even be favoured in the cases of binders B4 and B5, for which the hydration kinetics are slower because of the incorporation of slag and fly ash, respectively. More time is then available for the finer open pores in the aggregates to fill in with the aqueous phase of the paste

It is then possible to suppose that almost all of the open pore volume of the OD aggregates will be filled with the aqueous phase and then with hydrated paste after diffusion of the soluble species into the pores under a concentration gradient between the paste and the aggregates.

In the SSD condition, the water suction towards the aggregates is non-existent, or much less pronounced than in the OD state, since it is accepted that all of the accessible aggregate pores are already saturated with water according to the preparation protocol (see Section 2.3.1). The negative concentration gradients of ionic species in solution will cause their diffusion towards the aggregate pores and generate the precipitation of hydration products that will develop and grow in the available space. Accordingly, in the case of the SSD moisture state, it is also possible to assume that all of the accessible pore volume of the aggregates is filled with hydrated paste at 90 days of age.

In conclusion, the volume fraction, X, of unfilled granular pores tends towards a value close to 0 at the age of observation (90 days). Therefore, X was set to 0 (Fig. 8).

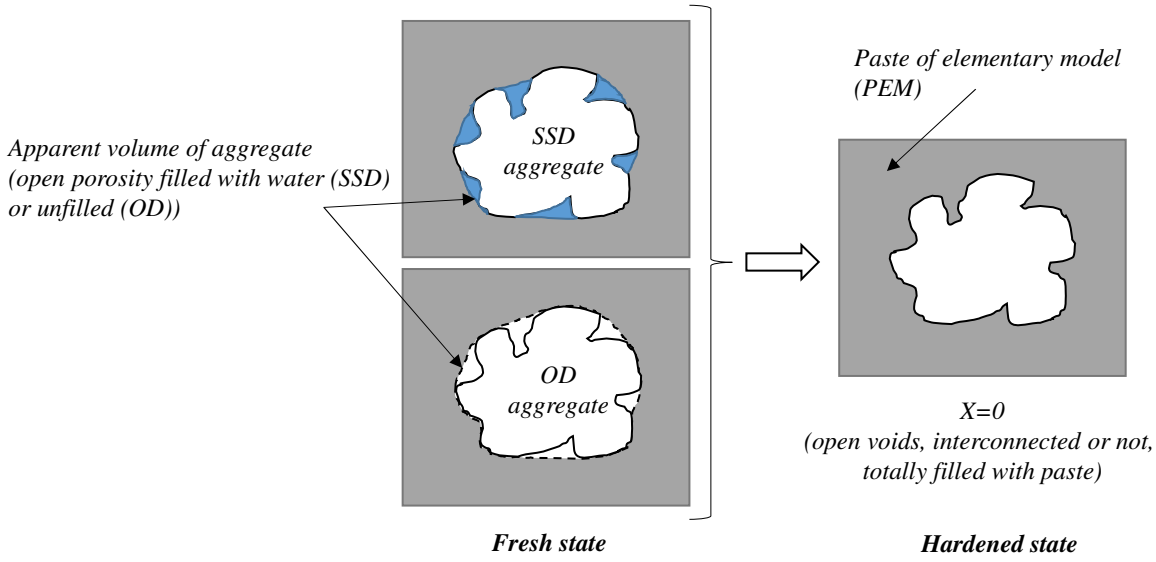

Fig. 8. Schematic illustration of the open porosity of aggregates becoming filled with paste in hardened EM (X=0) whatever the initial moisture state of aggregate (OD or SSD) in the fresh state of EM

Based on a preliminary study of the sensitivity of the results of WP^{PEM} to the variation of X, whatever the moisture state and the volume content of the aggregates may be, the choice X = 0 and the related analyses (Sections 4.1.3 and 4.1.4) are legitimate:

- over the entire range of variation of X ([0; 1]) for non-porous aggregates (G1, G2, G3) (Fig. 9a);
- up to X = 0.3 (30% of the unfilled granular volume) for porous aggregates (G4 and RA) (Fig. 9b).

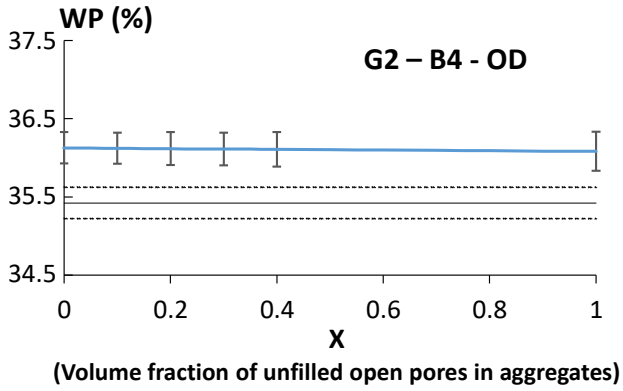

Typically, for low porous aggregate (G1, G2 and G3) the comparison between WP^{PEM} and WP^{BP} remains the same for any value of X ∈ [0 ; 1].

(a)

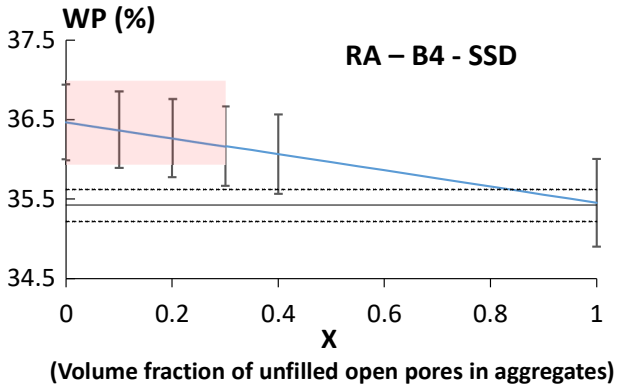

Typically, for porous aggregate (G4 and RA) the comparison between WP^{PEM} and WP^{BP} remains the same for X ∈ [0 ; 0.3] in the most extreme cases.

(b)

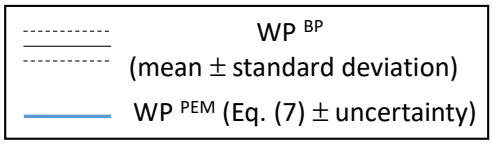

Fig. 9. Comparison between WP ^{PEM} and WP ^{BP} as a function of X. (a) Non-porous aggregates, (b) Porous aggregates – Aggregate volume content = 1V

4.1.3. Results of WP ^{PEM} (Volume content of aggregates = 1V)

The WP ^{PEM} values (mean ± uncertainty) calculated according to Eq. (7) and the WP ^{BP} values (mean ± standard deviation) obtained from measurements (Eq. (1)) on samples of hardened cementitious pastes are plotted in Fig. 10. The uncertainty on WP ^{PEM} is the maximal absolute uncertainty calculated from the experimental standard deviation values on WP ^{EM} (3 measurements), Γ_{agg} (3 measurements) and WP ^{agg} (10 measurements). It ranges from ± 0.1% to ± 0.5%, which corresponds to an accuracy (relative error) on WP ^{PEM} ranging from ± 0.3% to ± 1.3%.

Fig. 10 enables the paste porosity of EM samples, WP ^{PEM}, and the porosity of the plain bulk paste, WP ^{BP}, to be compared directly. The influence of the nature of the aggregates on the paste/aggregate interface can then be highlighted as a function of the nature of the binder and the moisture state of the aggregates. Table 6 shows the order relation between WP ^{PEM} and WP ^{BP} values for all the couplings (Gi; Bi) at a given moisture state (SSD or OD).

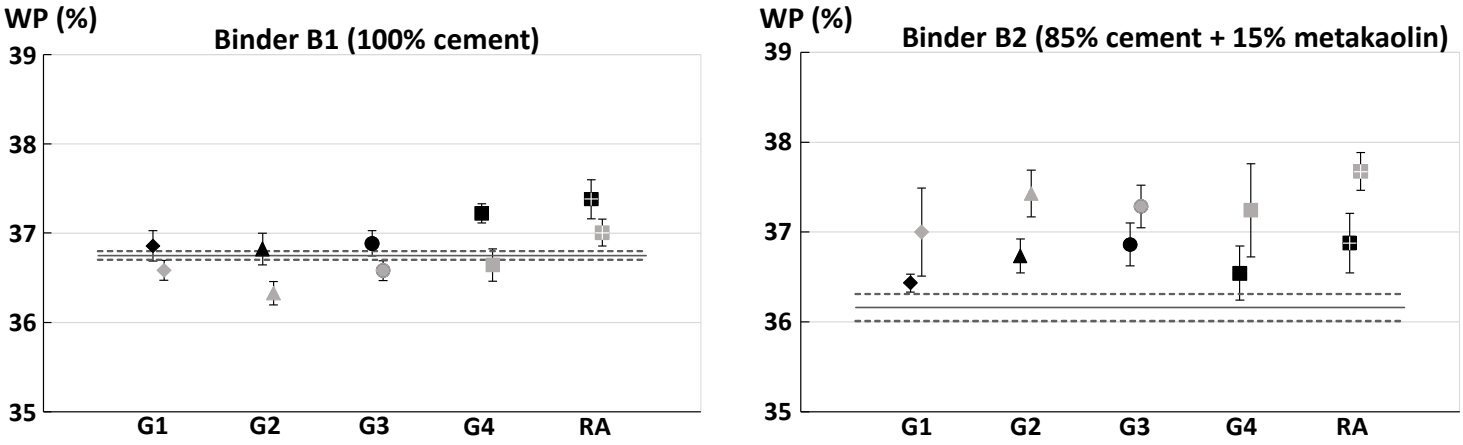

(a) (b)

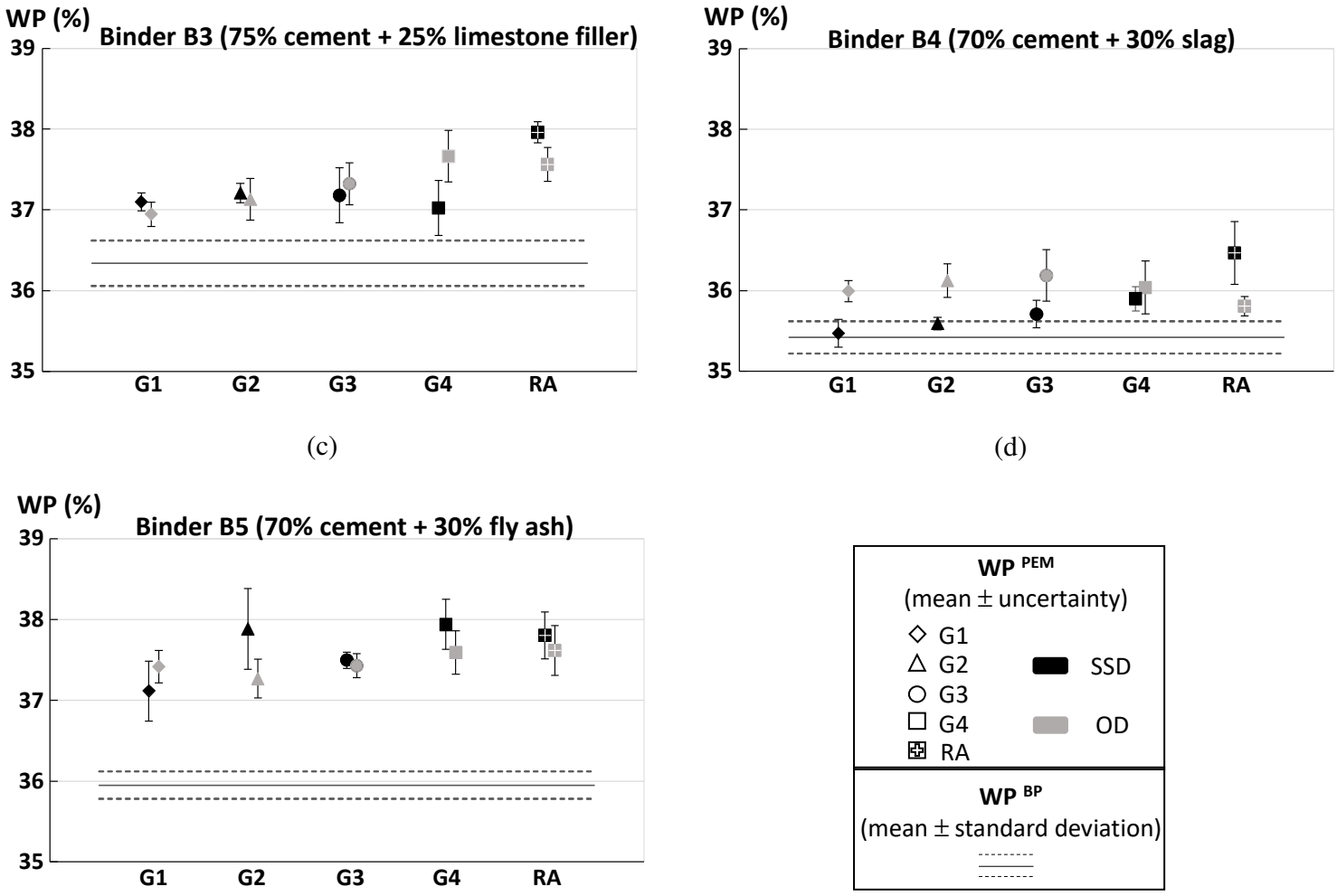

Fig. 10. Comparison between WP ^{PEM} values and WP ^{BP} values

Table 6. Order relationship between WP ^{PEM} and WP ^{BP} values

	G1		G2		G3		G4		RA		Tie
	SSD	OD	SSD	OD	SSD	OD	SSD	OD	SSD	OD	(row)
B1	=	=	=	<	=	=	>	=	>	>	6/10
B2	=	>	>	>	>	>	=	>	>	>	2/10
B3	>	>	>	>	>	>	>	>	>	>	0/10
B4	=	>	=	>	=	>	>	>	>	>	3/10
B5	>	>	>	>	>	>	>	>	>	>	0/10
Tie	4/10		2/10		3/10		2/10		0/10		Total
(column)	3	1	2	0	2	1	1	1	0	0	11/50

"=" means no significant difference; "< or >" means significant difference

a) First comments

Overall, 11 times out of 50, the aggregates appear to have no significant effect on the structuring of the paste. The "neutrality" of aggregates is mainly observed when low porous aggregates are used (9 times out of 11). The neutrality depends more on the moisture state than on the nature of the low porous aggregate (column tie in Table 6 for G1, G2 and G3) since there are more cases of equality in the SSD state than in OD state. Regarding porous aggregates, the only 2 cases of equality are for G4 in OD (SSD) state when combined with binder B1 (B2). Recycled aggregates RA always have an effect on the structuring of the surrounding paste.

The granular neutrality is much more contrasted, depending on the nature of the binder (line tie in Table 6):

- The cases of equality are the most numerous for B1 (6/10), B4 (3/10) and B2,

- There is no tied case for B3 and B5.

The other cases (39/50), for which the presence of aggregates is no longer neutral with respect to the structuring of the surrounding paste, are, as expected, predominant and are now discussed.

The occurrence $WP^{PEM} < WP^{BP}$ is observed very rarely and exclusively in the case of slightly porous to non-porous aggregates in the OD condition when they are associated with the non-composed B1 binder (G2 proven, trend for G1 and G3, see Fig. 10a). In contrast, the use of a composed binder (B2, B3, B4, or B5) in combination with porous or non-porous aggregates in the OD state induces WP^{PEM} values that are greater than those of WP^{BP}. Thus, the intensity of the gradient of water content from the fresh paste towards the aggregates and the structuring of the paste/aggregate interface do not depend only on the porosity of the aggregates but also on the reactivity of the binder, which is greater for B1 than for the other binders. The size of the capillaries of the paste B1 will then quickly decrease over time with the hydration development. The capillary suction forces will therefore have to be high at the same time to extract the water from the paste. In the case of B1, a state of equilibrium is then rapidly established, leading to a structuring of the paste/OD aggregate interface, which tends to be densified ($WP^{PEM} < WP^{BP}$) in the case of non-porous aggregates (low suction) and little affected ($WP^{PEM} = WP^{BP}$) in the case of porous aggregates (strong suction). For the other, less reactive binders, the reduction in capillary size due to hydration takes more time, allowing time for capillary suction to i) establish a higher water/binder ratio at the paste/OD aggregate interface when fresh, ii) enable higher porosity when hardened (Fig. 10b, Fig. 10c, Fig. 10d and Fig. 10e). However, before the setting phase, the water

retention capacity of the composed binders is different, depending on their fineness and the size distribution of their particles (see Section 4.1.2), also influences the structuring of the paste and should be considered in the analysis of the results (see Subsection b) below).

In the context of the elementary model EM, it is also important to mention that the use of porous aggregates in SSD state does not systematically improve the structuring of the paste/aggregate interface at the age of observation, in comparison with the OD condition. It is even an increase in porosity between the SSD state and the OD state that is observed when RA (G4) is associated with the binders B1, B3 and B4 (B1). The presence of water in the significant open porosity of G4 and RA results in the diffusion, under concentration gradient, of soluble species from the fresh paste. Such species have space to precipitate because the water/binder ratio is so high in the pore volume that the hydrates can easily grow and create a loose arrangement of the paste. If precipitation cannot occur because the concentrations of species are below the saturation level, and provided that the aggregate pores are larger than those in the surrounding paste, the pore solution released from the aggregates to the hydrating paste near the aggregate interface helps to maintain a high water/binder ratio, thereby causing high porosity.

The results obtained about the particular effect of the RA moisture state on the porosity of the matrix near the interface are finally in agreement with previous studies [32,33]. In Sidorova's work [32], by means of nanoindentation, it was not possible to distinguish different properties of the paste (cement only) near to or far from aggregate inserted dry into a given volume of paste. Djerbi [33] highlighted that high porosity existed over a 100-µm distance away from oversaturated aggregates in concretes made with cement+limestone filler. The results observed for the combination between G4 (calcareous aggregate with high porosity) and B1 binder are also in agreement with those of Nguyen et al. [56]. These authors showed that, for a given water/cement ratio, the ITZ is more porous in hardened mortars with oversaturated porous limestone aggregates than with the same aggregates used dry.

To close this section, for given binder and moisture state, it is clear that the results are not very dependent on the mineralogical nature of the aggregate when porosity is low (G1, G2 and G3) as they follow a similar trend. The differences between the composed binders are discussed in the following section.

b) Effect of composed binders on WP ^{PEM}

As implied above, the nature of the binder is definitely the parameter that most influences the structuring of the paste near the aggregate, porous or not. The case of B1 has been discussed above (Subsection a) and the behaviour of the composed binders deserves further analysis.

In the case of B3 and B5, the significantly higher porosity of the paste in presence of the aggregates depends little on the nature or the moisture state of the aggregates (Fig. 10c and Fig. 10e).

Concerning binder B3, as already observed by Wu et al. [27] with limestone and cement powders of similar fineness and median particle size to the ones studied here, the dilution effect at 10% replacement rate of cement with limestone filler dominates the physical and chemical mechanisms densifying the paste. The filler effect (improvement of the packing of the binder particles) and the nucleation effect (precipitation of smaller crystals of Portlandite with less preferential orientation) that occur with the incorporation of limestone filler are then lessened in comparison with the increase in the water to cement ratio caused by the dilution effect at 25% replacement rate. The prominent dilution effect, accentuated by the presence of aggregates (excess of water near the aggregates in the SSD state, suction of water from the paste towards the aggregates in the OD state) explains the more porous structuring of the paste in EM samples than in the bulk paste hydrated without aggregates.

Regarding now binder B5 (Fig. 10e), the literature shows that long curing time is needed to decrease the ITZ thickness and porosity [20], as well as to improve the ITZ bond [57]. Xu et al. [58] have shown that the pozzolanic reaction of Portlandite (CH) with the fly ash glass phase becomes significant after 28 days of hydration. Before, i.e. at early age, the replacement of cement with slow-reacting fly ash reduces the contact points between the matrix and the aggregates, and increases the water/cement ratio locally, which promotes the formation of Portlandite (CH) crystals. Furthermore, the slow hydration kinetics in the presence of fly ash is probably aggravated when the aqueous phase is significant close to the SSD aggregates or drained close to the dry OD aggregates. It follows that, at the age of observation (90 days), the microstructure has not yet densified enough. Furthermore, even if alkalis migrate to the transition zone [59], their contents in the cement used (0.76% K_2O and 0.28% Na_2O) are perhaps not high enough to enable significant dissolution of the fly ash at 90 days and the consumption of Portlandite. Particularly in the OD

state, the high WP PEM values are associated with a significant chemical variation over a greater distance from the aggregate, whatever its nature (Table 6).

In the case of binder B2 (Fig. 10b), the porosity WP PEM remains higher than that of the bulk paste WP BP, whatever the aggregate nature, but the SSD condition tends to improve the interface compactness in comparison with the OD condition. The effect of metakaolin (MK) on the decrease of the porous volume of the bulk paste through the pore refinement at later ages [2] is confirmed here when compared with the WP BP value of binder B1 (Fig. 10a). However, in the presence of aggregates, the porosity of the paste is adversely modified, especially when aggregates are in the OD moisture state. It has been shown that replacement of 20% of cement by mass with MK promotes the densification of the paste close to granite and limestone rocks by decreasing the amount and degree of orientation of Portlandite [60] and by decreasing the ITZ thickness [61]. The MK used here is not as fine or as pure (40% of quartz as a molar proportion of the mineralogical phase) as that used in the studies cited. Furthermore, it is important to consider the sensitivity of the MK and therefore of the binder B2 to the water available for the hydration of the cement. Near the aggregate, there are fewer coarse particles of cement and MK because of the wall effect and thus there is no interruption in the continuity of a large number of pores. Then, the drainage of the pore solution from the paste to the aggregates exists as long as the wall effect is significant. When the arrangement of the binder particles is no longer disturbed by the aggregate, the B2 paste is certainly the one where the water movement is the least intense in distance of all the composed binders, because the B2 binder has the greatest internal surface area (Table 1) and, at the same time, has coarse grains (Fig. 1). These two properties have the effect of reducing the initial size and number of capillaries in the paste [55], and synergistically increasing its water retention capacity. Since the amount of water available near the interface is not sufficient, the structuring of the paste is loose, with a greater porosity near the aggregate surface at later ages, irrespective of the porosity of the aggregates. The sensitivity of MK to water was highlighted in a previous study that showed no significant difference between the properties of the ITZ and the bulk paste in model mortars (paste-silicate glass beads) with high water/binder ratio (0.5 and 0.6) [62].

In the case of binder B4 (Fig. 10d), WP^{PEM} values are similar to WP^{BP} values when low-porous aggregates in SSD conditions are used but increase when the aggregates are in an OD state. In an association of B4 with porous aggregates, the increase in WP^{PEM} is effective for both moisture states but the OD state appears less deleterious than the SSD one in the case of recycled aggregates (RA). The incorporation of ground granulated blast furnace slag (GGBS) induces the smallest bulk

paste porosity (WP ^{BP}) in comparison with the other binders used, which confirms the positive effect of GGBS on the porosity of cementitious materials at later ages [63]. In the presence of aggregates, whatever their nature, and compared to the other binders, the porosity of the paste (WP ^{PEM}) remains low. As highlighted by previous studies [64,65], GGBS grains near the aggregate interface react (often later) with the local Portlandite crystals to form C-S-H hydrate with low C/S ratio. This new secondary C-S-H growth densifies the ITZ. However, the sensitivity of binder B4 to the aggregate moisture state is observed as for binder B2 (cement+metakaolin), yet to a lesser extent. Accordingly, the densification process of the paste/aggregate interface can be adversely affected if the water/cement ratio is initially high at the interface (case of porous aggregates in SSD state) or by the progressive increase of the water/cement ratio due to the suction of aggregates in the OD state before the setting phase. However, in the OD state, the WP ^{PEM} porosity does not seem to depend on the porosity of the aggregate. The low initial reactivity of the binder B4 associated with a low water retention capacity (low fineness and low D_{50} size) can induce a strong suction of the porous aggregates that extends over a large distance in the paste. This is not the case with low-porous aggregates, for which the suction remains localized at the interface. The more gradual water content gradient in the case of porous aggregates can induce a concentration of the pore solution below the saturation level over a great distance, which leaves a sufficient quantity of calcium ions available for the slag to react and help to limit the increase in porosity in EM samples.

At this stage, in the majority of combinations (aggregate; binder), it is possible to affirm that the aggregates modify the structuring of the paste when, for fixed water/binder ratio, the porosity of the paste in the presence of aggregates (WP ^{PEM}) and the porosity of the paste without aggregates (WP ^{BP}) are compared. It is the nature of the binder rather than the porosity of the aggregates that controls the results obtained on the porosity of the paste in the EM samples, WP ^{PEM}. The essential explanation lies in i) the capacity of the binder to retain water in reaction to the suction of dry aggregates (OD state) in the first hours after mixing, through its internal specific surface and its particle size distribution, and ii) its reactivity over time, which depends on the moisture state of the aggregates, porous or not.

The effect of increased aggregate volume content on WP ^{PEM} is discussed in Section 4.1.4. The representation of the results obtained (Sections 4.1.3 and 4.1.4) in terms of physical structuring of the paste near the aggregates is developed in Section 4.2.

4.1.4. Effect of the volume content of the aggregate on WP ^{PEM}

First of all, it is important to recall here that the volume of paste in the fresh state was fixed in the EM samples, whatever the volume content of aggregates (1V, 2V or 3V).

Secondly, regarding only the comparison between WP ^{PEM} and WP ^{BP}, it has been verified that the comments developed in the preceding section for one volume content of aggregates (1V) remain true for 2V and 3V, as shown in Fig. 11.

In a third step, it is interesting to analyse whether or not the increase in the volume of aggregates accentuates the observations made in the previous section. To that end, the WP ^{PEM} mean values corresponding to three volumes of aggregates in EM samples (3V), WP ^{PEM} - 3V, are plotted versus WP ^{PEM} - 1V values for the SSD moisture state (Fig. 12a) and for the OD moisture state (Fig. 12b). The equality line and its 95% confidence interval are also plotted on Fig. 12. The uncertainties on WP ^{PEM} are only plotted for points located outside the limits of the confidence interval, in order to directly verify whether the differences are significant or not.

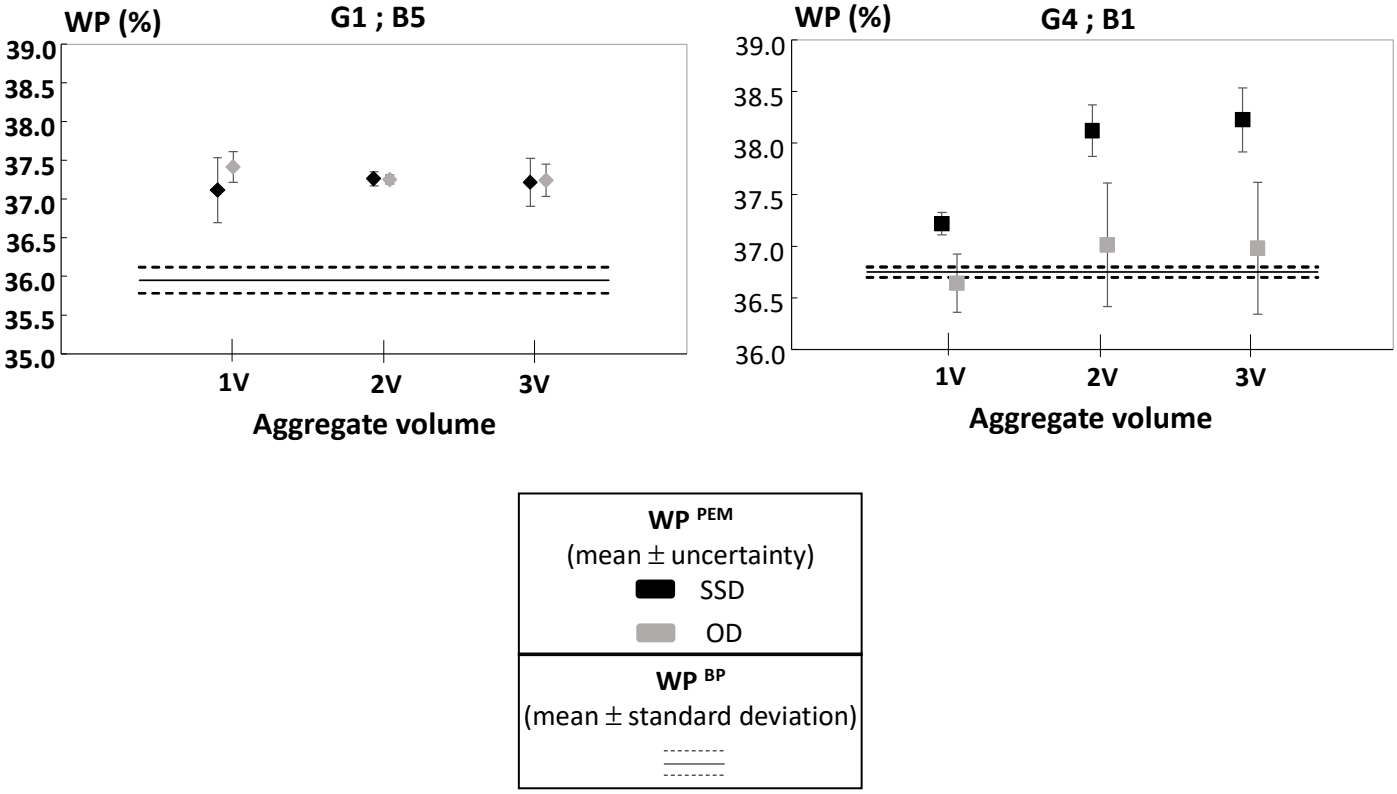

Fig. 11. Unchanged comparison between WP ^{PEM} and WP ^{BP} values according to the volume of aggregates – typical examples for low-porous aggregate (left) and porous aggregate (right)

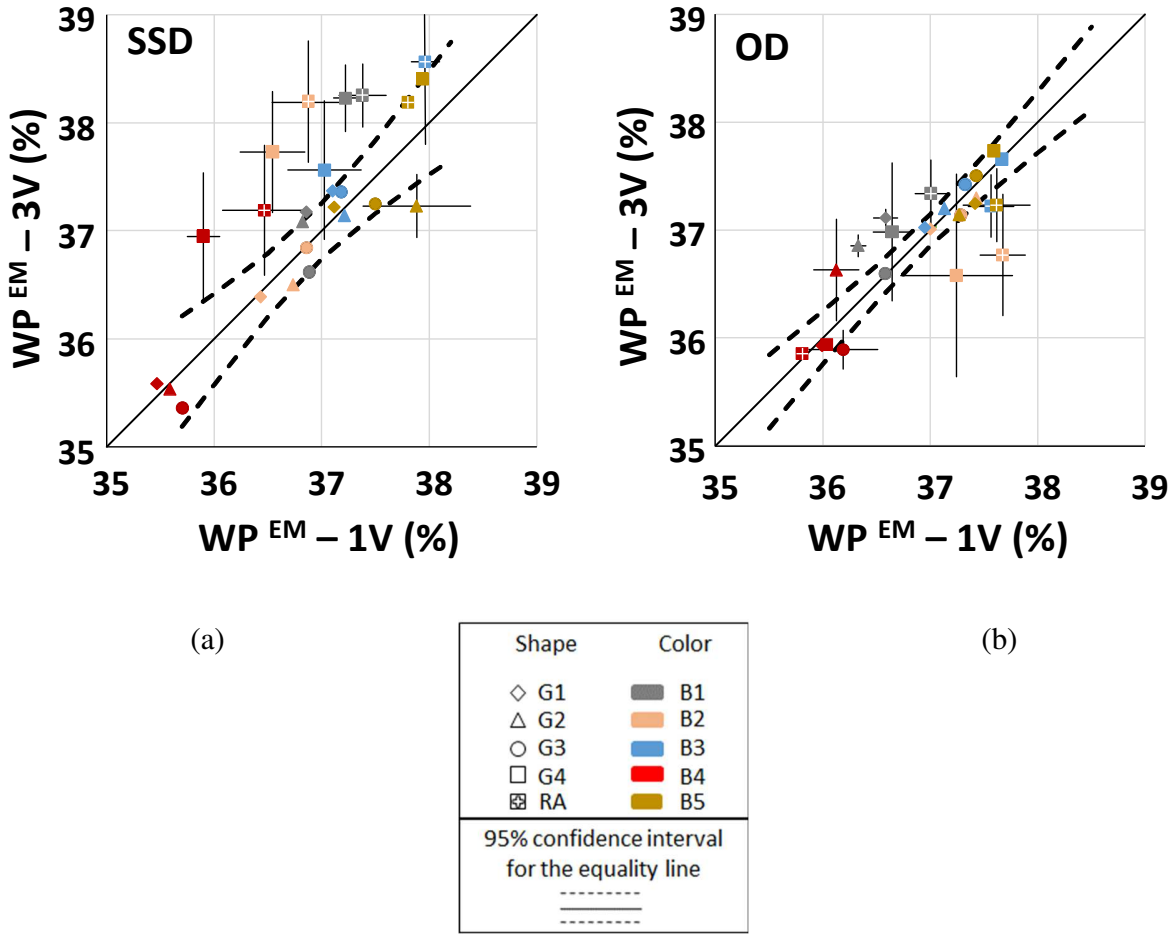

Fig. 12. WP ^{PEM} values for 3V aggregate volume content vs WP ^{PEM} values for 1V aggregate volume content – (a) SSD moisture state (a), (b) OD moisture state

The increase in the volume content of aggregates in the SSD state tends to accentuate the porosity of the paste in EM samples in the case of porous aggregates (the corresponding points are at the upper limit or above the 95% confidence interval, see Fig. 12a). It can be assumed that the supply of water resulting from the open porosity of the aggregates dilutes the paste in the vicinity of the aggregates and thus contributes, by increasing the water/cement ratio, to an increase in the porosity at the interface. It is important to note that, depending on the nature of the binder, the increase in porosity:

- becomes significant with the increase in volume from 1V to 3V in the case of binders B1 and B2;
- is never significant in the case of binders B3, B4 and B5.

When the porous aggregates are in the OD moisture state (Fig. 12b), it is observed that the increase in the aggregate volume content has little effect on the porosity of the paste; a reduction in porosity is observed in the case of binder B2, although it is not significant for G4. It is likely that the capillary suction of the water towards the aggregates is amplified with the increase in the aggregate volume, but is self limiting as it causes faster compaction of the paste. Then, the average size of the capillaries of the paste decreases very quickly and only the impregnation of the finest capillaries of the aggregates remains possible - but the volume represented by these capillaries remains low and therefore has little influence on the impregnation whether there are one or three volumes of aggregates.

In the case of non-porous aggregates, both in the SSD state (Fig. 12a) and the OD state (Fig. 12b), the incidence of the aggregate volume content on the porosity of the paste in EM at a given paste volume content very often remains low, or even zero, since the majority of the scatterplot is still included within the confidence interval. Only the increase in the volume content of the aggregates OD G1 and OD G2 associated with the binder B1 (cement only) causes a significant increase in porosity in the EM samples. The increase in the number of the paste/aggregate interfaces can lead to a marked loosening in the arrangement of the hydrates produced by the hydration of cement. This hypothesis is supported in the case of porous aggregates (G4, RA) combined with cement only when the corresponding points are also situated above the confidence interval (Fig. 12b).

4.2 Physical representation of the differences between WP^{PEM} and WP^{BP}: thickness e^{P}_{ITZ} of the interfacial zone between aggregates and the paste in EMs

4.2.1. Expression of the ITZ volume fraction: Γ_{ITZ}

Let $\Delta(X=0)$ be the difference between $WP^{PEM}(X=0)$ and WP^{BP} (the volume fraction, X, of unfilled open pores in aggregates is set to 0, see section 4.1.2). $\Delta(0)$ can represent the effect of the aggregates on the structuring of the paste.

When $\Delta(0) > 0$, the aggregates cause an increase in the porosity of the paste in EM. When $\Delta(0) = 0$, the arrangement of hydration products is not perturbed by the aggregates in EM. Finally, when $\Delta(0) < 0$, the aggregates cause a compaction of the paste in EM.

At this step, an attempt is made to express $\Delta(0)$ according to the following representation of EM.

Let us consider the EM as aggregates, each of them being surrounded by an ITZ of thickness e (i.e., e^{P}_{ITZ}), then by the bulk paste (Fig. 13). The thickness e^{P}_{ITZ} can be considered as the extent

of the perturbation in the structuring of the paste from the aggregate towards the bulk paste. This parameter may vary with the aggregate volume content.

This is a simple approach which should nevertheless provide a representative model of the structuring of the hydration products occurring at the paste/aggregate interfaces in EM samples.

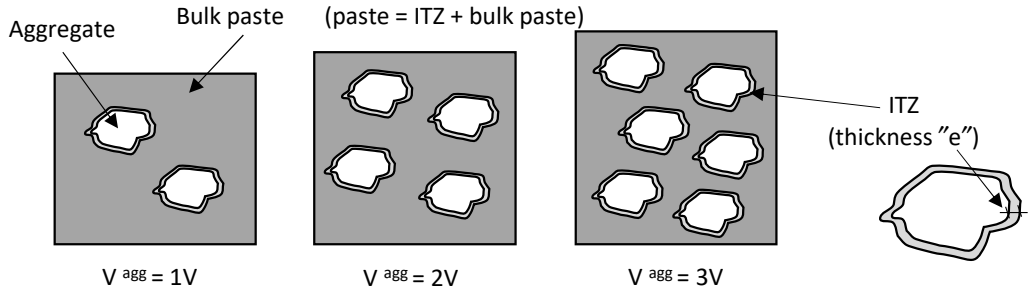

Fig. 13. Schematic representation of EM as a three-phase composite: aggregates, ITZ and bulk paste

Based on the EM representation in Fig. 13 and on Eq. (4), it is possible to write (Eq. (8)):

$$WP^{EM} = \frac{V_V^{PEM}(0)}{V^{EM}} = \frac{V_V{}^{ITZ}(0) + V_V{}^{BP}(0)}{V^{EM}} \quad (8)$$

where: $V_V{}^{ITZ}(0)$ and $V_V{}^{BP}(0)$ are the volumes of open voids in the ITZ and the bulk paste of EM for X=0. These volumes are part of the apparent volume of EM, V^{EM}.

Moreover, it is possible to express the ratio between $V_V{}^{BP}(0)$ and V^{EM} by considering that the open porosity of the bulk paste is WP^{BP} (Eq. (9)):

$$\frac{V_V{}^{BP}(0)}{V^{EM}} = \frac{V^{BP}(0) \,.\, WP^{BP}}{V^{EM}} \quad (9)$$

where: $V^{BP}(0)$ is the apparent volume of the bulk paste in EM, expressed in Eq. (10):

$$V^{BP}(0) = V^{EM} - V^{ITZ}(0) - V^{agg}(0) = V^{EM} - V^{ITZ}(0) - V^{agg}.\,(1 - WP^{agg}) \quad (10)$$

where: $V^{ITZ}(0)$ is the ITZ volume in EM samples for X=0.

Therefore, Eq. (9) can be written in a more explicit way (Eq. (11)):

$$\frac{V_V{}^{BP}(0)}{V^{EM}} = \left[1 - \Gamma_{ITZ}(0) - \Gamma_{agg}.\,(1 - WP^{agg})\right].WP^{BP} \quad (11)$$

where: $\Gamma_{ITZ}(0)$ is the volume fraction of the ITZ in EM ($i.e.$ $\frac{V^{ITZ}(0)}{V^{EM}}$).

The difference between Eq. (8) and Eq. (11) corresponds to the ITZ void volume fraction in EM and expresses, according to the model illustrated in Fig. 13, how the aggregates disturb the structuring of the paste near the interface. This difference finally has the same physical meaning

as $\Delta(0)$ and, if it were to take the same value as $\Delta(0)$, a related value could be given to $\Gamma_{ITZ}(0)$ according to Eq. (12):

$$\Gamma_{ITZ}(0) = \frac{\Delta(0) - WP^{EM}}{WP^{BP}} + 1 - \Gamma_{agg}(1 - WP^{agg}) \quad (12)$$

Based on this reasoning, all the parameters expressing $\Gamma_{ITZ}(0)$ are known and, if $\Delta(0) \geq 0$ (95% of cases), $\Gamma_{ITZ}(0)$ can be calculated from Eq. (12). Considering the mean $\Delta(0)$ values, $\Gamma_{ITZ}(0)$ ranges from 0.01% (0.01%) for V^{agg} = 1V to 0.8% (1.1%) for V^{agg} = 3V in the case of non-porous (porous) aggregates. As expected, even converted into volume fraction of the paste and due to the nature of the elementary model, these values are low in comparison with the ITZ volume fraction, which ranges from 30% to 50% of the total volume of the cement-based matrix in typical concrete systems [25].

For 5% of cases (exclusively binder B1 combined with non-porous aggregates or porous ones for the three-aggregate volume contents studied), the values of $\Delta(0)$ are negative and Eq. (12) gives negative values for $\Gamma_{ITZ}(0)$, which does not make sense. However, this does not mean that there is no ITZ in EM as variations in calcium content and Ca/Si ratios are observed near the interface in all EM samples (see Table 5, Section 3.2). Then, the meaning of the representation of EM (Fig. 13) is also maintained by considering a more compact structure in the ITZ volume than in the bulk paste volume when $\Delta(0) < 0$. For the sake of comparison with the majority of cases and as illustrated in Fig. 14, the volume fraction of compact ITZ is calculated using Eq. (12) from the absolute value of $\Delta(0)$, i.e. as if $\Delta(0)$ was positive.

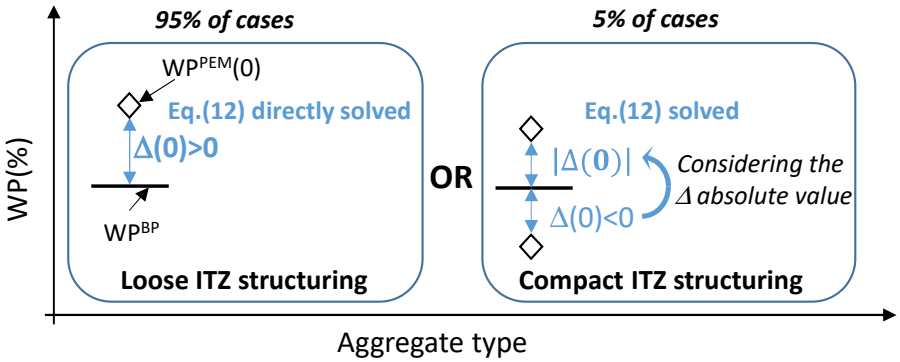

Fig. 14. Solving Eq. (12) according to the sign of $\Delta(0)$

4.2.2. ITZ thickness: e^{P}_{ITZ}

In order to determine the ITZ thickness, representing the extent of the change in the arrangement of the hydration products from the aggregate towards the bulk paste, an expression for $\Gamma_{ITZ}(0)$ different from the one defined by Eq. (12) is needed.

The concept developed by Lu and Torquato [66] enables Γ_{ITZ} to be expressed (Eq. (13)) by considering a polydisperse system of hard spheres in a matrix. Each sphere is randomly placed in the matrix according to equilibrium statistics, i.e. as if spheres were free to take a desired position in the matrix. According to Lu and Torquato, if a shell of a given thickness surrounds each of the spheres, it is possible to define the volume fraction of material outside the spheres and their associated shells. The concept was applied by Garboczi and Bentz [67] to assess the influence of the ITZ on some mechanical and physical concrete properties analytically and Eq. (13) is directly derived from Garboczi and Bentz's study. The concept was also applied by Radovskiy [68] to analytically determine the volume fraction of air voids in compacted asphalt mixture and the asphalt shell thickness for any combination of aggregates and asphalt matrix. In concrete applications [67], Eq. (13) works very well provided that gravitational settling is not severe, that there is a large size distribution of aggregates and that the aggregates are round. In addition, Eq. (13) remains quite successful for a monodispersed system of particles. Since EM can be considered as monodispersed round aggregates suspended in cementitious matrix with significant resistance to segregation at small volume fraction in EM (Γ_{agg} ranges from 7% (1V - aggregate content) to 19% (3V - aggregate content)), Eq. (13) can be applied in the present study under satisfactory conditions.

$$\Gamma_{ITZ}(0) = \left[1 - \Gamma_{agg}(0)\right] - \left[1 - \Gamma_{agg}(0)\right].e^{-\pi\rho(ce+de^2+ge^3)} \quad (13)$$

where: $e = e^{P}_{ITZ}$ = thickness of the shell surrounding each aggregate,

$\Gamma_{agg}(0)$ = aggregate volume fraction when the open pores of the aggregates are completely filled with paste,

ρ = number density of aggregates in EM, i.e. number of aggregates per unit volume of EM.

c, d and g are the following defined quantities:

$$c = \frac{4<R^2agg>}{1-\Gamma_{agg}(0)}$$

$$d = \frac{4<R_{agg}>}{1-\Gamma_{agg}(0)} + \frac{12z_2<R^2agg>}{[1-\Gamma_{agg}(0)]^2}$$

$$g = \frac{4}{3[1-\Gamma_{agg}(0)]} + \frac{8z_2<R_{agg}>}{[1-\Gamma_{agg}(0)]^2} + \frac{16Az_2^2<R^2_{agg}>}{3[1-\Gamma_{agg}(0)]^3}$$

where: <Ragg>, <R²agg> are number averages of the aggregate radii and their squares, respectively,

A: is a parameter equal to 0 in the context of cementitious material [67].

$$z_2 = \frac{2\pi\rho<R^2_{agg}>}{3}$$

In the present study, by considering the selected aggregates incorporated in EM as spherical particles (Section 2.1.2a), <Ragg> and <R^2agg> were calculated in the [14-16]-mm size class belonging to the size distribution of each of the coarse aggregates studied. They verify the conservation of the volume and the number of particles in the [14-16]-mm size class and are closely representative of the volume and the number of aggregates in EMs.

The equality between Eq. (12) and Eq. (13) makes it possible to write a cubic equation in the ITZ thickness e= e^{P}_{ITZ} (Eq. (14)):

$$ce + de^2 + ge^3 = \left[\frac{-1}{\pi\rho}\right].ln\left[\frac{WP^{EM} - \Delta(0)}{WP^{BP}(1-\Gamma_{agg}(0))}\right] \quad (14)$$

The ITZ thickness is found as the real root of Eq. (14).

4.2.3 Results

a) Comparison between ITZ physical thickness e^{P}_{ITZ} *and* e^{M}_{ITZ} *(aggregate volume content = 1V)*

The ITZ physical thickness e^{P}_{ITZ} calculated according to Section 4.2.2 is plotted versus the measured ITZ chemical width (e^{M}_{ITZ}, Section 3.2), together with the equality line (Fig. 15).

Irrespective of the aggregate moisture state, e^{P}_{ITZ} is most often larger than e^{M}_{ITZ}. Accordingly, based on the EM representation (Fig. 13), the arrangement of the hydration products, rather than their chemical change analysed from Ca and Si contents, is disturbed over a greater distance from the aggregate. The physical disturbance can reach or exceed 100 µm and can be most often related to a loose structuring of the ITZ in which large crystallised hydration products have developed.

In the SSD condition, this trend is always verified in the case of porous aggregates (G4 and RA, Fig. 15a), while, in the OD moisture state (Fig. 15b), it depends on the nature of the binder: similar values between e^{P}_{ITZ} and e^{M}_{ITZ} are observed for B1 (G4 and RA) and for B4 (RA only).

As expected from the results discussed in Section 4.1.3, the physical disturbance is particularly marked in the case of binders B3 (cement + limestone filler) and B5 (cement + fly ash) whatever the nature and the moisture state of the aggregates.

Furthermore, it is worth mentioning that the sensitivity of binder B2 (cement + metakaolin) to the moisture state of aggregates, irrespective of their nature, is remarkable: the OD moisture state implies larger disturbance from the aggregates of the (loose) structuring of the paste (Fig. 13b). This trend also exists for binder B4 (cement + slag) but is dependent on the nature of the aggregates. In the particular case of RA, the physical disturbance is similar to the e^{M}_{ITZ} in the OD condition.

While it is not explicit in Table 5 (Section 3.2), Fig. 15 also shows that the scatterplot is more dispersed in the OD state than in SSD state in the case of binders B2 and B4. The influence of the aggregate nature on e^{M}_{ITZ} is therefore highlighted.

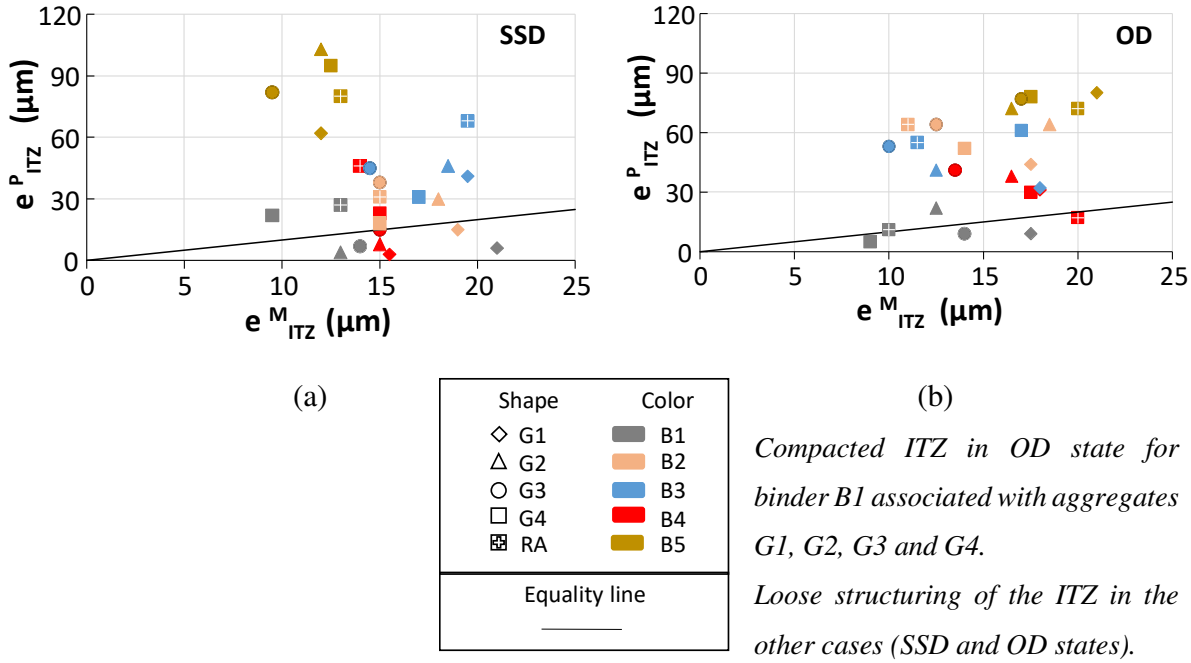

Compacted ITZ in OD state for binder B1 associated with aggregates G1, G2, G3 and G4.

Loose structuring of the ITZ in the other cases (SSD and OD states).

Fig. 15. ITZ physical thickness e^{P}_{ITZ} vs. chemical thickness e^{M}_{ITZ}
(a) SSD moisture state, (b) OD moisture state

b) Effect of the aggregate volume content on the ITZ physical thickness

The mean values of physical thickness corresponding to three volumes of aggregates in EM samples (3V), "e^{P}_{ITZ} - 3V", are plotted versus "e^{P}_{ITZ} - 1V" mean values for the SSD moisture state (Fig. 16a) and for the OD moisture state (Fig. 16b). The equality line and its 95% confidence interval are also plotted on Fig. 16.

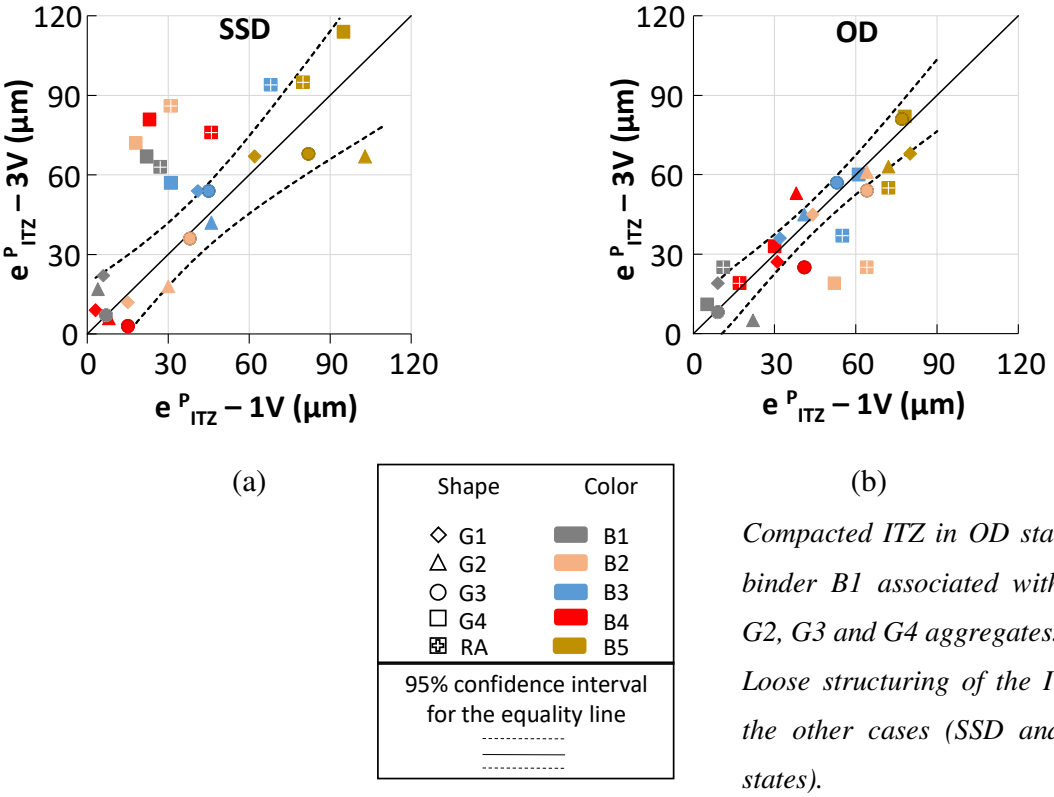

Compacted ITZ in OD state for binder B1 associated with G1, G2, G3 and G4 aggregates. Loose structuring of the ITZ in the other cases (SSD and OD states).

Fig. 16. Physical ITZ thickness for 3V aggregate volume content vs physical ITZ thickness for 1V aggregate volume content – (a) SSD moisture state, (b) OD moisture state

In the SSD condition, the increase in the aggregate volume content tends to extend the disturbance of the arrangement of the hydration products in the case of porous aggregates, since the corresponding points are situated near or above the upper limit of the confidence interval (Fig. 16a). Conversely, for non-porous aggregates, the related scatterplot remains included within the confidence interval and it can be concluded that the increase in the aggregate volume content does not significantly modify the thickness of the ITZ.

In the OD condition (Fig. 16b), the ITZ thickness is not affected by the increase in the aggregate volume content for most cases. Nevertheless, for porous aggregates, the extent of the physical disturbance decreases with the increasing aggregate volume content, particularly when they are combined with B2 binder.

5 Conclusions

This paper, as a preliminary step to investigations at the concrete scale, is dedicated to the study on elementary models (EM), composed with paste and various volume contents of coarse aggregates (1V, 2V or 3V) with a view to enhancing the phenomena occurring at the paste

aggregate interface. In addition to the aggregate volume content, the study parameters were the nature (porous or not), the moisture state (SSD, OD) of the aggregates and the nature of the binder (cement only, cement combined with limestone filler or metakaolin, or ground granulated blast furnace slag or low-calcium fly ash).

After 90-days of water curing, the water porosity of EM (WP^{EM}) and the chemical width of the interfacial transition zone (e^{M}_{ITZ}) were measured.

- The following results are noteworthy. Typically, irrespective of the nature of the binder, WP^{EM} values are higher with aggregates in the SSD moisture state than in the OD state, particularly when i) porous aggregates are incorporated and ii) the aggregate volume content increases. Observation i) is in agreement with previous literature results obtained on composite model, vibrated mortar and vibrated concrete.
- The e^{M}_{ITZ} values mainly range from 10 µm to 20 µm - the same order of magnitude as, or significantly lower than, the median size of the binders.
- By dispensing with the strong dependence of WP^{EM} on the aggregate porosity, the porosity of the paste in the elementary model (WP^{PEM}) was calculated to better highlight the coupling between the nature of the aggregate (OD or SSD moisture state) and the nature of the binder. Having justified that the majority of the accessible pore volume of the porous aggregates is filled with paste, the comparison, at a fixed water/binder ratio, between the porosity WP^{PEM} and the porosity of the paste without aggregates (WP^{BP}) enables it to be affirmed that:
  - The aggregates (porous or not) cause a loose structuring of the paste in the majority of combinations of {aggregate; binder}.
  - It is the nature of the binder rather than the porosity of the aggregates that controls the results obtained on the porosity of the paste in the EM samples, WP^{PEM}. The essential parameter derives from i) the capacity of the binder to retain water in reaction to the suction of dry aggregates (OD state) in the first hours after mixing, through its internal specific surface and its particle size distribution, ii) its reactivity over time, which depends on the moisture state of the aggregates (porous or not).
- The increase in the volume content of aggregates at a fixed paste content:
  - does not change the above conclusions on the comparison between WP^{PEM} and WP^{BP}.
  - tends to increase the WP^{PEM} values when porous (recycled and natural) aggregates are incorporated in the SSD condition but has little effect on WP^{PEM} when incorporated in the OD state.
  - remains insignificant when low-porous aggregates are used, whatever the moisture state may be.

➢ By representing the elementary model EM as a three-phase composite, i.e. aggregates, ITZ and bulk paste, and by considering the differences between WP^{PEM} and WP^{BP}, the ITZ volume fraction was calculated. The satisfactory approximation of modelling EM as hard spheres suspended in a matrix, each of the spheres being surrounded by a matrix shell of given thickness, enabled physical ITZ thicknesses e^{P}_{ITZ} to also be calculated from the previously determined ITZ volume fractions. It was shown that:

- irrespective of the aggregate moisture state, the thickness e^{P}_{ITZ} was most often larger than the ITZ chemical width e^{M}_{ITZ}, i.e. it is the (most often loose) arrangement of the hydration products rather than their chemical change that is disturbed over a greater distance from the aggregate. The physical disturbance has a 40 µm median value but can punctually reach 100 µm.
- There is no order relation between e^{P}_{ITZ} and e^{m}_{ITZ}, i.e. a greater distance of chemical variation from the aggregate is not always associated with a larger difference in the arrangement of hydrates between the ITZ and the bulk paste, depending on the aggregate moisture state and the binder nature.
- The increase in the aggregate volume content does not systematically cause a variation (decrease or increase) in e^{P}_{ITZ}. The variation actually depends on the {aggregate; binder} combination for a given aggregate moisture state. It is noteworthy that, in the particular case of SSD for porous aggregates associated with any binder, the ITZ thickness e^{P}_{ITZ} always increases (a maximal (average) multiplying factor of 4 (2) is observed).

6 References

[1] Cassagnabère, F., Mouret, M., Escadeillas, G., Broilliard, P., Bertrand, A. (2010). Metakaolin, a solution for the precast industry to limit the clinker content in concrete: Mechanical aspects. Construction and Building Materials 24(7) 1109-1118.

[2] Duan, P. S., Shui, Z., Chen, W., Shen, C. 2013. Effects of metakaolin, silica fume and slag on pore structure, interfacial transition zone and compressive strength of concrete. Construction and Building Materials, 44, 1-6.

[3] Agrela, F., Alaejos, P., De Juan, M. S. 2013. Properties of concrete with recycled aggregates. In Handbook of recycled concrete and demolition waste. Dublin, Ireland: Woodhead Publishing.

[4] Marinković, S. B., Ignjatović, I. S., Radonjanin, V. S., Malešev, M. M. 2012. Recycled aggregate concrete for structural use–an overview of technologies, properties and applications. Dordrecht, Netherlands: Springer.

[5] Nilsen, A. U., Monteiro, P. J. M. 1993. Concrete: a three phase material. Cement and Concrete Research 147-151.

[6] Farran, J. 1956. Mineralogical contribution to the study of the adhesion between hydrated constituents of cements and coated materials. Rev. Mater. Constr 490-491, 155; 492, 191.

[7] Farran, J., Maso, J. C. 1964. The use of limestone substitutions for the improvement of concrete aggregates. Rev. Mater. Constr. 587-588, technical publication #156, 1-27

[8] Iwasaki, N., Tomiyama, Y. 1974. Microstructures and strength of interface between cement paste and aggregate. Rev. 29th Gen. Mtg., Cem. Assoc., Japan, 88-91.
[9] Barnes, B.D., Diamond, S., Dolch, W. L. 1979. Micromorphology of the interfacial zone around aggregates in Portland cement mortar. J. Am. Cer. Soc. 62(1-2) 21-24.
[10] Grandet, J., Ollivier J.P. 1980. Orientation of hydration products near aggregate surfaces. Proceedings of the 7th international Congress on the chemistry of cement, vol. III, (Editions Septima, Paris.) VII-63-VII-68.
[11] Scrivener, K., Pratt, P.L. 1986. A preliminary study of the microstructure of the cement/sand bond in mortars. Proceedings of the 8th international Congress on the chemistry of cement, vol. III, 466-471.
[12] Maso, J. C. 1980. The bond between aggregates and hydrated cement paste. Proceedings of the 7th international Congress on the chemistry of cement, vol. I (Editions Septima, Paris) VII-1/4-VII-1/15.
[13] Wu, Z. W., Liu, B. Y., Xie S. S. 1982. Interfacial zones in cement-based materials. Proceedings of international seminar on Liaisons pâtes de ciment matériaux associés (Imprimerie centrale de l'Artois.) A28-32.
[14] Bentz, D.P., Garboczi, J.,Stutzman, P. E. 1993. Computer modelling of the interfacial zone in concrete. In Maso J.C. (Ed.), RILEM Proceedings 18 on Interfaces in cementitious composites, (E&FN SPON) 107-116.
[15] Scrivener, K. L., Crumbie, A. K., Laugesen, P. 2004. The interfacial transition zone (ITZ) between cement paste and aggregate in concrete. Interface science 12.4 411-42
[16] Xie, Y., Corr, D.J., Jin, F., Zhou, H., Shah, S.P. 2015. Experimental study of the interfacial transition zone (ITZ) of model rock-filled concrete (RFC). Cem. Conc. Comp. 55, 223-231.
[17] Lyu, K., Garboczi, E.J., She, W., Miao, C. 2019. The effect of rough vs. smooth aggregate surfaces on the characteristics of the interfacial transition zone. Cem. Conc. Comp. 99, 49-61.
[18] Elsharief, A., Cohen, M.D., Olek, J. 2003. Influence of aggregate size, water cement ratio and age on the microstructure of the interfacial transition zone. Cem. Conc. Res. 33(11) 1837-1849.
[19] Simeonov, P., Ahmad S. 1995. Effect of transition zone on the elastic behavior of cement-based composites. Cem. Conc. Res. 25(1) 165-176.
[20] Mehta, P.K., Monteiro, P.J.M. 1987. Effect of aggregate, cement, and mineral admixtures on the microstructure of the transition zone, in S. Mindness and S.P. Shah (eds) MRS Proceedings 114 on bonding in cementitious materials. 65-75.
[21] Jiang, L. 1999. The interfacial zone and bond strength between aggregates and cement pastes incorporating high volumes of fly ash. Cement and Concrete Composites 21(4) 313-316.
[22] Cheng-yi, H., Feldman, R.F. 1985. Influence of silica fume on the microstructural development in cement mortars. Cement and Concrete research 15(2) 285-294.
[23] Goldman, A., Bentur, A. 1989. Bond effects in high strength silica-fume concretes. ACI Materials Journal 86(5) 440-447.
[24] Xuan, D.X., Shui, Z.H., Wu, S.P. 2009. Influence of silica fume on the interfacial bond between aggregate and matrix in near-surface layer of concrete. Construction and Building Materials 23(7) 2631-2635.
[25] Larbi, J.A. 1991. The cement paste-aggregate interfacial zone in concrete. PhD of the Delft University of Technology.
[26] Detwiler, R., Krishnan, K., Mehta, P.K. 1986. Effect of blast furnace slag on the transition zone in concrete, in B. and K. Mather (Eds). Proceedings ACI SP 100-6 on durability of concrete, vol.1, 63-72.
[27] Wu, K., Shi, H., Xu, L., Ye, G., De Schutter, G. 2016. Microstructural characterization of ITZ in blended cement concretes and its relation to transport properties. Cement and Concrete Research 79 243-256.
[28] Liu, S., Yan, P. 2010. Effect of limestone powder on microstructure of concrete. Journal of Wuhan University of Technology-Mater. Sci 25(2) 328-331.
[29] Mortureux, B., Hornain, H., Regourd, M. 1982. Cement paste-fillers bond in blended cements. Proceedings of international seminar on Liaisons pâtes de ciment matériaux associés (Imprimerie centrale de l'Artois.) A64-72.
[30] Zhang, M.H., Gjorv, O. E. 1990. Microstructure of the interfacial zone between lightweight aggregate and cement paste. Cement and Concrete Research 20(4) 610-618.

[31] Elsharief, A., Cohen, M. D., Olek, J. 2005. Influence of lightweight aggregate on the microstructure and durability of mortar. Cement and Concrete Research 35(7) 1368-1376.
[32] Sidorova, A., Vazquez-Ramonich, E., Barra-Bizinotto, M., Roa-Rovira, J.J., Jimenez-Pique, E. 2014. Study of the recycled aggregates nature's influence on the aggregate-cement paste interface and ITZ. Construction and Building Materials 68 677-684.
[33] Djerbi, A. 2018. Effect of recycled coarse aggregate on the new interfacial transition zone concrete. Construction and Building Materials 190 1023-1033.
[34] Bentz, D. P., Weiss, W. J. 2011. Internal curing: A 2010 State-of-the-art review. Gaithersburg: US Department of Commerce, National Institute of Standards and Technology.
[35] Scrivener, K.L., Gartner, E.M. 1987. Microstructural gradients in cement paste around aggregate particles, in S. Mindness and S.P. shah (Eds). MRS Proceedings 114 on bonding in cementitious materials 77-85.
[36] Bentur, A., Alexander, M.G. 2000. A review of the work of the RILEM TC159-ETC: engineering of the interfacial transition zone in cementitious composites. Materials and Structures 33 82-87.
[37] NF EN 197-1. 2012. Cement - Part 1: composition, specifications et conformity criteria for common cements, AFNOR Editions.
[38] NF P18-513. 2012. Addition for concrete - Métakaolin - Specifications and conformity criteria, AFNOR Editions.
[39] NF P18-508. 2012. Additions for concrete - Limestone additions - Specifications and conformity criteria, AFNOR Editions.
[40] NF EN 15167-1, 2006. Ground granulatd blast furnace slag for use in concrete, mortar and grout- Part 1: definitions, specifications and conformity criteria, AFNOR Editions.
[41] NF EN 450-1. 2012. Fly ash for concrete - Part 1: definition, specifications and conformity criteria, AFNOR Editions.
[42] NF P18-545. 2011. Aggregates - Defining elements, conformity and coding. AFNOR Editions.
[43] NF EN 1097-6, 2014: Tests for mechanical and physical properties of aggregates - Part 6: Determination of particle density and water absorption, AFNOR Editions.
[44] NF P18-459. 2010. Concrete – Testing hardened concrete – Testing porosity and density, AFNOR Editions.
[45] NF EN 206/CN. 2014. Concrete – Specification, performance, production and conformity. National addition to the standard NF EN 206, AFNOR Editions.
[46] De Larrard, F. 1999. Concrete mixture proportioning: a scientific approach. London: E&FN SPON.
[47] NF EN 196-1. 2016. Methods of testing cement Partie 1 : Détermination of strength, AFNOR Editions.
[48] Yuan, C.Z., Guo, W.J. 1987. Effect of bond strength between aggregate and cernent paste on the mechanical behaviour of concrete, in S. Mindess and S. P. Shah (Eds). MRS Proceedings 114 on bonding in cementitious materials 41-47.
[49] Yuan, C.Z., Odler, I. 1987. The interfacial zone between marble and tricalcium silicate paste. Cement and Concrete Research 17(5) 784-792.
[50] Sheskin, D. J. 2000. Parametric and nonparametric statistical procedures. Boca Raton: 4th edn. : Chapman and Hall/CRC.
[51] Jouenne, C.A. 1960. General Ceramics. Notions of physico-chemistry, tome II. Gauthier-Villars publisher, Paris, 408p (in french).
[52] Török, Á., Szemerey-Kiss, B. 2019. Freeze-thaw durability of repair mortars and porous limestone: compatibility issues. Progress in Earth and Planetary Science, 6(1) 42.
[53] Kayyali, O. 1987. Porosity of concrete in relation to the nature of the paste-aggregate interface. Materials and Structures 20, 19-26.
[54] Kim, Y.Y., Lee, K.M., Bang, J.W., Kwon, S.J. 2014. Effect of W/C ratio on durability and porosity in cement mortar with constant cement amount. Advances in materials science and engineering,. https://doi.org/10.1155/2014/273460.
[55] Grandet, J. 1975. Contribution to the study of the setting and carbonation of mortars in contact with porous materials. Toulouse, France: PhD thesis, Université Paul Sabatier, Toulouse.

[56] Nguyen, T.D., le Saout, G., Devillers, P, Garcia-Diaz, E. 2014. The effect of limestone aggregate porosity and saturation degree on the interfacial zone. 2nd International Symposium on Cement-Based Materials For Nuclear Waste (NUWCEM 2014), Avignon, France, 1-13.
[57] Wong, Y.L., Lam, L., Poon, C.S., Zhou, F.P. 1999. Properties of fly ash-modified cement mortar-aggregate interfaces. Cement and Concrete Research 29. 1905-1913.
[58] Xu, A., Sarkar, S. L., Nilsson, L. O. 1993. Effect of fly ash on the microstructure of cement mortar. Materials and Structures, 26(7) 414-424.
[59] Breton, D., Carles-Gibergues, A., Ballivy, G., Grandet, J. 1993. Contribution to the formation mechanism of the transition zone between rock-cement paste. Cement and Concrete Research, 23(2) 335-346.
[60] Bijen, J.M., Larbi, J. A. 1990. Effects of pozzolans on the aggregate-cement interface in relation to alkali-silica reaction. Proceedings of the Advanced Seminar on Alkali-Silica Reaction in Concrete, University of London, United Kingdom, 1-15.
[61] Larbi, J.A., Bijen, J.M. 1992. Influence of pozzolans on the Portland cement paste–aggregate interface in relation to diffusion of ions and water absorption in concrete. Cement and Concrete Research 22 551-562.
[62] Asbridge, A.H., Page, C.L., Page, M.M. 2002. Effects of metakaolin, water/binder ratio and interfacial transition zones on the microhardness of cement mortars. Cement and Concrete Research 32(9) 1365-1369.
[63] Li, Y., Chen, Y. 2006. Influence of ground mineral admixtures on pore structure of hardened cement paste and strength of cement mortar. Journal of the Chinese Ceramic Society 34(5) 575-579.
[64] Saito, M. Kawamura M. 1989. Effect of fly ash and slag on the interfacial zone between cement and aggregate, in Fly Ash, Silica Fume, and Natural Pozzolans in Concrete, SP-114, v.1,. American Concrete Institute, Detroit: 669–688.
[65] Hooton, R.D. 2000. Canadian use of ground granulated blast-furnace slag as a supplementary cementing material for enhanced performance of concrete. Canadian Journal of civil engineering 27(4) 754-760.
[66] Lu, B., Torquato, S. 1992. Nearest-surface distribution functions for polydispersed particle systems. Physical Review A 45(8) 5530-5544.
[67] Garboczi, E.J., Bentz, D.P. 1997. Analytical formulas for interfacial transition zone properties. Advances in Cement-Based Materials 6. 99-108.
[68] Radovskiy, B. 2003. Analytical formulas for film thickness in compacted asphalt mixture. Transportation Research Record 1829 (1) 26-32.

7 Abbreviations

EM = Elementary model (paste + coarse aggregates)
V^{agg} = apparent aggregate volume content = 1V (2 aggregate particles) or 2V (4 particles) or 3V (6 particles)
WP^{EM} = water porosity of EM (measured)
WP^{PEM} = water porosity of the paste in EM (calculated)
WP^{BP} = water porosity of the bulk paste (measured without aggregates)
WP^{agg} = water porosity of aggregates (measured)
SSD = saturated surface dry moisture state
OD = oven dry moisture state
Γ_{agg} = volume fraction of aggregates in EM
Γ_{ITZ} = volume fraction of ITZ in EM
X = volume fraction of open pores unfilled with paste
e^{P}_{ITZ} = calculated physical thickness of ITZ
e^{M}_{ITZ} = measured (SEM-EDS) chemical thickness of ITZ